Spikes in Poissonian quantum trajectories

Alan Sherry [1,*] Cedric Bernardin [2,†] Abhishek Dhar [1,‡] Aritra Kundu [3,§] and Raphael Chetrite [4,‖]

[1] *International Centre for Theoretical Sciences, Tata Institute of Fundamental Research, Bangalore 560089, India*

[2] *Faculty of Mathematics, National Research University Higher School of Economics, 6 Usacheva, Moscow 119048, Russia*

[3] *Department of Physics and Materials Science, University of Luxembourg, L-1511 Luxembourg*

[4] *Institut de Physique de Nice (INPHYNI), Université Côte d'Azur, CNRS, 17 rue Julien Lauprêtre, Nice 06200, France*

(Received 30 November 2024; accepted 1 April 2025; published 23 April 2025)

We consider the dynamics of a continuously monitored qubit in the limit of strong measurement rate where the quantum trajectory is described by a stochastic master equation with Poisson noise. Such limits are expected to give rise to quantum jumps between the pointer states associated with the nondemolition measurement. A surprising discovery in earlier work [A. Tilloy *et al.*, Phys. Rev. A **92**, 052111 (2015)] on quantum trajectories with Brownian noise was the phenomena of spikes observed in-between the quantum jumps. Here, we show that spikes are observed also for Poisson noise. We consider three cases where the nondemolition is broken by adding, to the basic strong measurement dynamics, either unitary evolution or thermal noise or additional measurements. We present a complete analysis of the spike and jump statistics for all three cases using the fact that the dynamics effectively corresponds to that of stochastic resetting. We provide numerical results to support our analytic results.

DOI: 10.1103/PhysRevA.111.042215

I. INTRODUCTION

In the last decade, the flourishing interest in feedback control of quantum systems has led to a renaissance of the theory of quantum measurements through continuous measurements. The cornerstone of continuous quantum measurements is the stochastic master equation (SME), also called the quantum trajectories equation, or the Belavkin-Barchielli equation. After an initial period of development in the spontaneous collapse community [1–4], SME was really born in the 1980s in quantum optics and quantum filtering communities [5–18]. They are now part of standard textbooks [19–24], and have been observed experimentally [25–30]. In the context of the so-called quantum nondemolition (QND) setup it is assumed that measurement operators, and possible Hamiltonians, are all diagonalizable in the same orthonormal basis, called the pointer basis. One of the most striking results in this case is that the large time-limiting form of the density matrix is in accordance with the usual Born rule. This has been observed experimentally [25–27] and proven theoretically in [31–35].

An interesting situation arises when one considers the non-QND setup (see Sec. II), where a lot of attention has recently been given to the case of large rate measurement limit, which is also called the strong collapse limit (or weak non-QND limit) of non-QND quantum trajectories. We then expect to see the emergence of quantum jumps between pointer states and this has been observed experimentally [36–38]. It was recently theoretically explained in [39] for SME with Gaussian noise in the collapse-thermal and collapse-unitary setups [40] generalized [39] for SME with Gaussian noise, in more general setups, particularly the collapse-measurement case. Reference [41] also discusses it for SME with Poisson noise in the collapse-unitary setup. Note that the quantum Zeno effect [42–47] argues that continuously observing a quantum state leads to a zero probability of evolving away from a given state, thus freezing the evolution of the system and suppressing the quantum jumps. However, the Zeno effect can be avoided if one considers the appropriate limit of system probe interactions.

A surprising discovery was the observation of sharp scale-invariant fluctuations that invariably decorate the jump process [see Figs. 1(c), 2(c), and 3(c)], in the limit where the measurement rate is very large. These seemingly instantaneous excursions have been referred to as *quantum spikes*. These fluctuations around the dominant jump process seem to be visible in the early numerical work on the subject [48–51]. A heuristic description was provided in [50,51], while their first analytical treatment was done recently by Bauer-Bernard-Tilloy [52–54], which motivated some other works [55,56]. Previous work has been exclusively concerned with Gaussian noise SMEs and explains these phenomena by relating it to the fact that the convergence to the jump process between pointer states is weak. However, this is expected to be valid for more general SMEs and we quote Tilloy [57]: *"A first possible generalization is to go from a continuous collapse model to a discrete one, and replace the diffusive equations we had with jump ones ... . However, while spikes are numerically present as well in this context and seem to have the exact same power law statistics, no proof is known even for the qubit case."* The

*Contact author: alan.sherry@icts.res.in
†Contact author: sedric.bernardin@gmail.com
‡Contact author: abhishek.dhar@icts.res.in
§Contact author: aritra.kundu@uni.lu
‖Contact author: raphael.chetrite@univ-cotedazur.fr

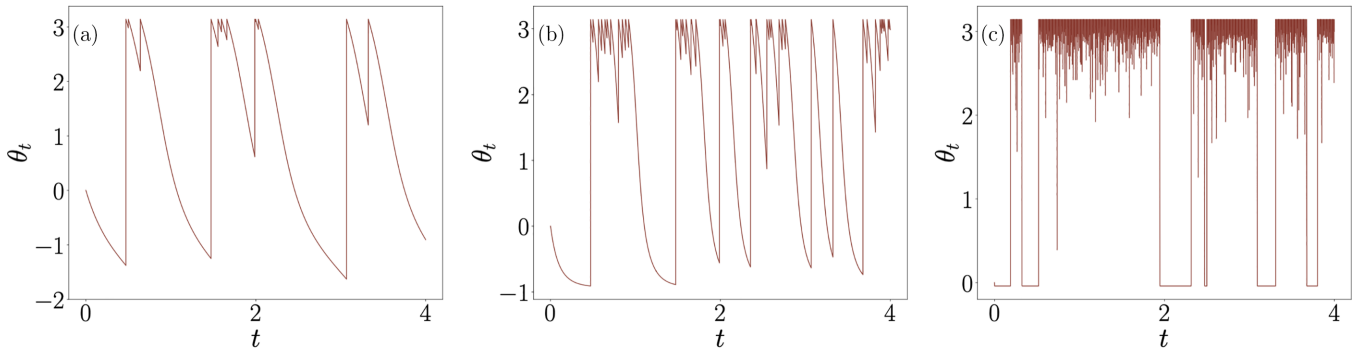

FIG. 1. Collapse-unitary setup: typical trajectories generated by Eq. (18) for increasing values of $\gamma_1 = 7, 25, 10\,000$ for (a), (b), (c), respectively, with the Rabi frequency tuned as $k_{\gamma_1} = \sqrt{\omega\gamma_1}$. In (a) we see time segments with a downward deterministic flow from π and then an upward vertical instantaneous reset to π: this constitutes a prespike. With increasing γ_1, these prespikes either form a jump to $\theta \approx 0$ or, more often, develop into spikes. Thus, we finally see in (c) a structure consisting of jumps (flows from π to $\theta \approx 0$ or instantaneous resets from $\theta \approx 0$ to π), interspersed with spikes emerging from the state $\theta = \pi$. After a jump to $\theta \approx 0$, the quantum trajectory remains here for a time $\sim 1/(4\omega)$ during which no spikes occur. In the simulations we took $\omega = 1$ and a time step $dt = 10^{-5}$ for iterating the Poisson process.

main goal of this paper is to demonstrate the phenomena of quantum spikes for the case of Poisson noise SMEs and to study their statistical properties.

We limit our analytical study to particular cases of a qubit system, for the three setups which we refer to as the collapse-unitary setup, the collapse-thermal setup, and the collapse-measurement setup. The restriction of our study, apart from the fact that it concerns only a qubit, is that its analytical resolution is based on the fact that the resulting dynamics is in fact a one-dimensional piecewise resetting Markov dynamics [58–61], and explicit Laplace transforms lead to the complete statistics of the associated quantum spikes. In Sec. VI we discuss our results in the context of more general piecewise deterministic Markov processes (PDMP).

The plan of the paper is as follows: In Sec. II, we discuss the general setup and then in Sec. III, explain the three specific models that we study here. In Sec. IV, we summarize the main results and present comparisons of various analytic expressions with numerical data. The mathematical derivations are presented in Sec. V. In Sec. VI, we enlarge our discussion for more abstract mathematical models and state a conjecture about the spikes statistics for the latter. We conclude the paper with a conclusion section (see Sec. VII), where we also discuss the relevance of spikes in real experimental studies.

II. GENERAL SETUP: STOCHASTIC MASTER EQUATION (SME) OF *d*-DIMENSIONAL SYSTEMS WITH POISSON NOISE

We consider here SMEs with Poisson white noise (discarding the possible Gaussian part of the noise), in finite d-dimensional Hilbert space, describing the real-time evolution of a quantum system with (Hermitian) density matrix ρ [$\rho \geqslant 0, \mathrm{Tr}(\rho) = 1$] with free evolution given by a Hermitian Hamiltonian H, thermal evolution given by a Lindbladian L^{th} [62,63], and simultaneous independent continuous measurement of p operators $\{N_k \in \mathcal{M}_d(\mathbb{C})\}_{k=1,\ldots,p}$, where $\mathcal{M}_d(\mathbb{C})$ denotes the set of square complex matrices of size d, and with rate of measurement $\gamma = \{\gamma_k\}_{k=1,\ldots,p}$. The evolution equation of the density matrix is given by the PDMP [see, for

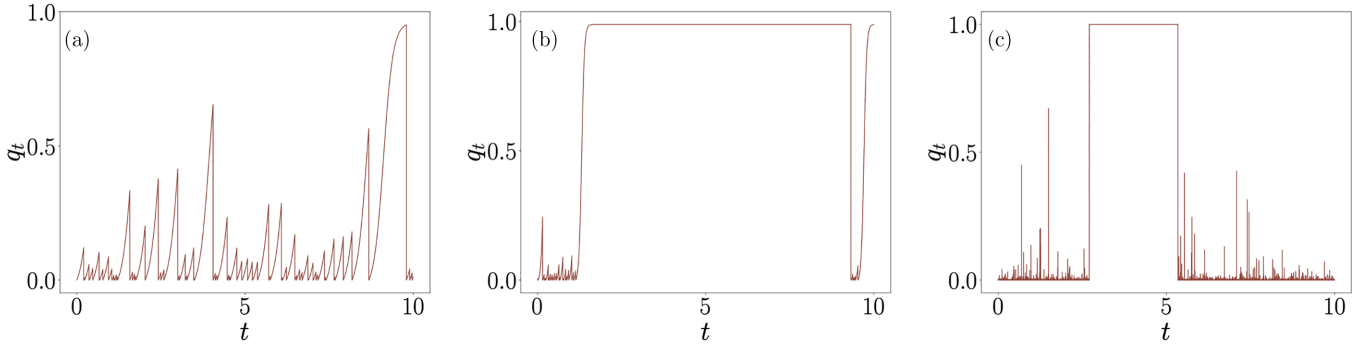

FIG. 2. Collapse-thermal setup: typical trajectories generated by Eq. (20) for different values of $\gamma_1 = 7, 25, 10\,000$ for (a), (b), (c), respectively. Here we see that in (a), the trajectory has time segments with prespikes which consist of an upward deterministic flow from $q = 0$, and a downward reset to the state $q = 0$. In the large-γ_1 limit in (c), the prespikes develop into sharp spikes and we again see an effective Poisson jump process between the pointer states at $q = 0$ and 1, decorated by spikes emerging from the lower branch. The parameters here are $W_{\mp} = W_{\pm} = 0.3$, $\eta_1 = 1$, $dt = 10^{-5}$.

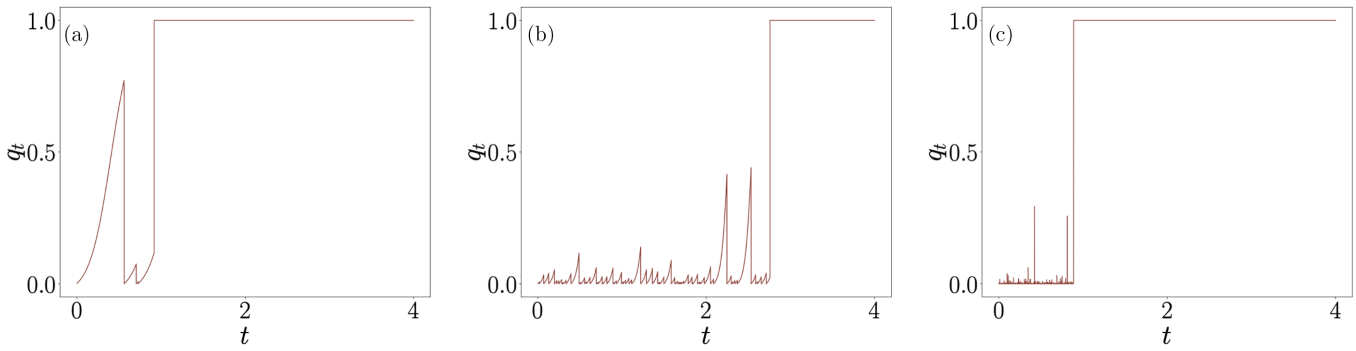

FIG. 3. Collapse-measurement setup: typical trajectories from Eq. (23) for increasing values of $\gamma_1 = 7,\ 25,\ 10\,000$ for (a), (b), (c), respectively. In this case the prespikes have the same form as in Fig. 2 and again we see spikes emerging in the limit of large γ_1. However, in this case, the spikes are transient since one has a vanishing transition rate from $q = 1$ to 0. The parameters are $\gamma_2 = 1.0$, $\eta_1 = 1.0$, $\eta_2 = 0.7$, $dt = 10^{-5}$.

example, relations (6.224)–(6.227) of [22]]

$$\dot{\rho}_t^{\gamma} = -i\big[H, \rho_t^{\gamma}\big] + L^{th}\big[\rho_t^{\gamma}\big] + \sum_{k=1}^{p}\Big\{\gamma_k L_{N_k}\big[\rho_t^{\gamma}\big] + M_{N_k}\big[\rho_t^{\gamma}\big]\big[\dot{\mathcal{N}}_t^{k,\gamma} - \mathbb{E}\big(\dot{\mathcal{N}}_t^{k,\gamma}\big|\rho_t^{\gamma}\big)\big]\Big\}\,. \tag{1}$$

In the previous equation, note the following:

(i) The (classical) *signal measurements* $\{\mathcal{N}_t^{k,\gamma}\}_{k=1,\dots p}$ are given by nonautonomous Poissonian processes ($d\mathcal{N}_t^{k,\gamma} \in \{0, 1\}$ and $d\mathcal{N}_t^{k,\gamma} d\mathcal{N}_t^{\ell,\gamma} = d\mathcal{N}_t^{k,\gamma}\delta_{k\ell}$), with statistics

$$\mathbb{E}\big(d\mathcal{N}_t^{k,\gamma}\big|\rho_t^{\gamma}\big) = \gamma_k\eta_k \mathrm{Tr}\big(N_k\rho_t^{\gamma}N_k^{\dagger}\big)dt. \tag{2}$$

We will refer to the signals $d\mathcal{N}_t^{k,\gamma} = 1$ as "clicks." Note that, in all the terms, ρ_t^{γ} in the previous equations must be understood as the density matrix taken just before an eventual jump happening at time t.

(ii) The *measurement operators* N_k are arbitrary matrices (not necessarily commuting, not necessarily Hermitian) and characterize each independent detector. The parameters $\eta_k \in [0, 1]$ are the associated detector efficiencies: $\eta_k = 1$ (respectively $\eta_k = 0$) corresponds to a perfect efficient detector (respectively an unread measurement).

(iii) The *Lindbladian*[1] operator L_N, associated to the measurement operator N, encapsulates the back effect of the N measurement on the average evolution. It is given by [62,63]

$$L_N[\rho] = N\rho N^{\dagger} - \tfrac{1}{2}N^{\dagger}N\rho - \tfrac{1}{2}\rho N^{\dagger}N. \tag{3}$$

(iv) The *stochastic innovation* $M_N[\rho]$ is the nonlinear operator defined by

$$M_N[\rho] = \frac{N\rho N^{\dagger}}{\mathrm{Tr}(N\rho N^{\dagger})} - \rho. \tag{4}$$

From a theoretical viewpoint, the simplest way to derive the SME (1) from ideal physical systems is as the limit of infinitely frequent indirect measurements (with the system-ancilla interaction becoming infinitely strong in the limit) (see, for example, [20,22,24,64–66]). The nonlinearity in Eq. (1) is a remnant of the nonlinear updating of all types of Bayesian measurements. However, this nonlinearity is in fact the effect of the fixed normalization $\mathrm{Tr}(\rho_t^{\gamma}) = 1$ since, without this normalization, Eq. (1) can be formulated as a linear equation [19–24].

Note that in practice, for a real experiment, the knowledge about the quantum system is only stored in the Poisson signal process $\{\mathcal{N}_t^{k,\gamma}\}_{k\in1,\dots,p}$. The density matrix ρ_t^{γ} itself is not directly observable, and is only reconstructed from the Poisson signal process.

A. Large-time limit of the SME equation (1): To collapse or not

The first crucial question concerning the SME equation (1) is the understanding of its large-time behavior. Let us assume for the moment that we do not have any thermal bath $L^{th} = 0$. The *quantum nondemolition (QND)* hypothesis [20,21,25,67–72] is the fact that there exists an orthonormal basis $\{|e_i\rangle\}_{i=1,\dots,d}$, called the *pointer basis* [73], such that all the measurement operators $\{N_k\}_{k=1,\dots,p}$, and the Hamiltonian H, are diagonal in this basis. Under this hypothesis (and a nondegeneracy condition that we do not discuss here, see [35]), the large-time limit of the density matrix in Eq. (1) is given by the famous collapse-absorbing formula

$$\lim_{t\to\infty}\rho_t^{\gamma} = |e_i\rangle\langle e_i| \text{ with probability } \big\langle e_i, \rho_0^{\gamma}e_i\big\rangle. \tag{5}$$

This corresponds to the Born rule for measurement outcomes under projective measurements of any of the N_k at the initial time. Related results have been observed experimentally [25–27] and are proven theoretically in [31–35].

However, there are many ways to break the QND hypothesis, and we discuss three different ones:

(1) *Collapse-unitary setup*. We may allow that the Hamiltonian H is not diagonal in the pointer basis $\{|e_i\rangle\}_{i=1,\dots,d}$ related to the measurement operators $\{N_k\}_{k=1,\dots,p}$. It results then in a competition between collapse in the pointer basis and a unitary evolution (noncollapsing) generated by H.

(2) *Collapse-thermal setup*. We may take into account the thermal interactions with the external world, i.e., $L^{th} \neq 0$. Then it results in a competition between collapse equation (5) in the pointer basis, and, thermalization towards a Gibbs state.

(3) *Collapse-measurement setup*. We may allow that one of the measurement operators, say N_p, is not diagonal in the pointer basis $\{|e_i\rangle\}_{i=1,\dots,d}$ related to $\{H, \{N_k\}_{k\neq p}\}$. It results

[1]Completely positive trace-preserving map from $M_d(\mathbb{C})$ to $M_d(\mathbb{C})$.

then in a competition between collapse equation (5) in the pointer basis of $\{H, \{N_k\}_{k\neq p}\}$ and collapse in the pointer basis related to N_p, if N_p is diagonalizable. If N_p is not diagonalizable, there is competition between collapse in the pointer basis related to $\{H, \{N_k\}_{k\neq p}\}$ and the uncollapse dynamics generated by the measurement operator N_p.

In all these three setups, the large-time collapse equation (5) is then *a priori* broken.

B. Strong collapse Zeno limit in a non-QND setup: Quantum jump phenomenon versus spikes phenomenon

In this work, instead of the large-time limit we consider the large γ strong collapse limit, also called the quasi-Zeno limit. For non-QND quantum trajectories, Eq. (1) leads to a richer phenomenology:

(i) *Quantum jumps*. The expected quantum jumps definitively arise between the pointer basis. More formally, the density matrix will converge to a pure jump Markov process

$$\lim_{\gamma\to\infty} \rho_t^\gamma = |X_t\rangle\langle X_t|, \tag{6}$$

where $X_t \in \{|e_i\rangle\}_{i=1,\dots,d}$ is a pure jump Markov process with explicit computable rates [39–41]. In some cases they can vanish. For example, the transition rate between pointer states decreases as $\frac{1}{|\gamma|}$ for large γ in the collapse-unitary setup, for a fixed H (this is reminiscent of the Zeno effect).

(ii) *Quantum spikes*. One finds that sharp scale-invariant fluctuations invariably decorate the jump process [see Figs. 1(c), 2(c) and 3(c) below], in the limit where the measurement rate is very large. We call *quantum spikes* these seemingly instantaneous excursions. These spikes become infinitely thin when $\gamma \to \infty$, i.e., take a time $\frac{1}{|\gamma|}$ while their heights remain of order 1 in the limit. As discussed above, such spikes have been observed and explained for the case with Gaussian noise [52–54]. These articles explain the spiking phenomena as the fact that the convergence in Eq. (6) is weak. Exporting these methods in the present context seems to be a difficult task since the authors there are using tools specific to Brownian motion.

III. PRECISE SETUP: SME OF QUBIT FOR NONDEMOLITION "RESET" CONTINUOUS MEASUREMENT OF $|-\rangle\langle -|$

We consider a qubit system with basis $\{|+\rangle, |-\rangle\}$, where continuous collapse measurement competes with a thermal, another measurement, or a unitary dynamics. Precisely, we consider the collapse measurement of a rank-one diagonal (see QND hypothesis) operator

$$N_1 = \begin{pmatrix} 0 & 0 \\ 0 & 1 \end{pmatrix} = |-\rangle\langle -|. \tag{7}$$

The jumps in the SME equation (1) due to the term $M_{N_1}[\rho_t^\gamma]\dot{\mathcal{N}}_t^{1,\gamma}$ are, thanks to Eq. (4), given by

$$\rho \to \rho + M_{N_1}[\rho] = \frac{N_1\rho N_1^\dagger}{\mathrm{Tr}(N_1\rho N_1^\dagger)} = |-\rangle\langle -|, \tag{8}$$

i.e., the result after the jump is always the same matrix, irrespective of the state just before the jump: this is a resetting dynamics [58–61]. In fact, the crucial property to get resetting dynamics is not the precise form of N_1 but the fact that the matrix N_1 is of rank one ("sharp measurement"). Since we are considering a qubit, note also that the only other rank-one diagonal measurement operator satisfying QND hypothesis is

$$\begin{pmatrix} 1 & 0 \\ 0 & 0 \end{pmatrix} = |+\rangle\langle +|, \tag{9}$$

which gives exactly the same theory by the exchange $|+\rangle \to |-\rangle$. Hence, our focus will be on N_1. Note that in Sec. VI, we will discuss an extension to general diagonal N_1.

By parametrizing the density matrix as usual as

$$\rho_t^\gamma = \begin{pmatrix} q_t^\gamma & \overline{u}_t^\gamma \\ u_t^\gamma & 1-q_t^\gamma \end{pmatrix}, \tag{10}$$

with $(q_t^\gamma, u_t^\gamma) \in \mathbb{R}\times\mathbb{C}$, we get explicitly in Appendix A the analytical form of the N_1-measurement part [in the SME equation (1)] for general diagonal N_1. For the particular case (7), it takes the form of a three-dimensional process:

$$\begin{aligned} \dot{q}_t^\gamma &= -q_t^\gamma\big(\dot{\mathcal{N}}_t^{1,\gamma} - \gamma_1\eta_1(1-q_t^\gamma)\big), \\ \dot{u}_t^\gamma &= -\frac{\gamma_1}{2}u_t^\gamma - u_t^\gamma\big(\dot{\mathcal{N}}_t^{1,\gamma} - \gamma_1\eta_1(1-q_t^\gamma)\big) \end{aligned} \tag{11}$$

with

$$\mathbb{E}\big(d\mathcal{N}_t^{1,\gamma}\big|q_t^\gamma\big) = \gamma_1\eta_1(1-q_t^\gamma)dt, \quad d\mathcal{N}_t^{1,\gamma}d\mathcal{N}_t^{1,\gamma} = d\mathcal{N}_t^{1,\gamma}.$$

Note that the resetting Eq. (8) corresponds in the coordinates (10) to the resetting to $(q=0, u=0)$. Moreover the equations in Eq. (11) show that the population q_t^γ is a martingale collapsing to $\{0, 1\}$ [31–35,74]. Moreover, in average, u_t^γ shrinks trivially to zero at large time, or for strong measurement $\gamma_1 \to \infty$ (decoherence). We will study analytically three specific cases where we add either a unitary drive or a thermal bath or a noncommuting measurement.

A. Collapse-unitary setup: Measurement of Rabi qubit coherent oscillations

We choose here no extra measurement apart from N_1, and

$$L^{th} = 0, \quad H = k_{\gamma_1}\sigma_x = k_{\gamma_1}\begin{pmatrix} 0 & 1 \\ 1 & 0 \end{pmatrix}. \tag{12}$$

This Rabi Hamiltonian H and the measurement operator N_1 given in Eq. (7) do not commute and then, they are not diagonalizable in a common orthonormal basis. Moreover, the *ad hoc* dependency in γ_1 of the Rabi frequency k_{γ_1} (which is, in general, proportional to the magnetic field) will stay unfixed for the moment, and will be discussed below in relation to the quantum Zeno effect. The Hamiltonian contribution is given by

$$-i\big[H, \rho_t^\gamma\big] = -ik_{\gamma_1}\begin{pmatrix} u_t^\gamma - \overline{u}_t^\gamma & 1-2q_t^\gamma \\ 2q_t^\gamma - 1 & \overline{u}_t^\gamma - u_t^\gamma \end{pmatrix}, \tag{13}$$

and the SME equation (1) takes then the form of a three-dimensional PDMP

$$\begin{aligned} \dot{q}_t^\gamma &= -ik_{\gamma_1}\big(u_t^\gamma - \overline{u}_t^\gamma\big) - q_t^\gamma\big(\dot{\mathcal{N}}_t^{1,\gamma} - \gamma_1\eta_1(1-q_t^\gamma)\big), \\ \dot{u}_t^\gamma &= -ik_{\gamma_1}\big(2q_t^\gamma - 1\big) - \frac{\gamma_1}{2}u_t^\gamma - u_t^\gamma\big(\dot{\mathcal{N}}_t^{1,\gamma} - \gamma_1\eta_1(1-q_t^\gamma)\big) \end{aligned} \tag{14}$$

with

$$\mathbb{E}\big(d\mathcal{N}_t^{1,\gamma}\big|q_t^\gamma\big)=\gamma_1\eta_1\big(1-q_t^\gamma\big)dt,\quad d\mathcal{N}_t^{1,\gamma}d\mathcal{N}_t^{1,\gamma}=d\mathcal{N}_t^{1,\gamma}.$$

Note that contrary to the collapse-thermal setup and the collapse-collapse setup, discussed in the following two sections, the real population q_t^γ is not autonomous: it depends of the complex coherence u_t^γ. Finally, when the rate of measurement vanishes (i.e., $\gamma_1=0$), this is the usual equation for Rabi oscillation [75,76]: precession of a spin $\frac{1}{2}$ in an external magnetic field.

Parametrize now the density matrix in Bloch coordinates:

$$\rho_t^\gamma=\frac{1}{2}\begin{pmatrix}1+r_t^\gamma\big(\cos\theta_t^\gamma\big) & r_t^\gamma\big(\sin\theta_t^\gamma\big)\exp\big(-i\varphi_t^\gamma\big)\\ r_t^\gamma\big(\sin\theta_t^\gamma\big)\exp\big(i\varphi_t^\gamma\big) & 1-r_t^\gamma\big(\cos\theta_t^\gamma\big)\end{pmatrix},\tag{15}$$

with[2]

$$0\leqslant r_t^\gamma\leqslant 1,\quad \theta_t^\gamma\in\,]-\pi,\pi],\quad \varphi_t^\gamma\in[0,\pi].\tag{16}$$

We show in Appendix C, Eq. (C1), that in the totally efficient case $\eta_1=1$, Bloch sphere of pure states $r_t^\gamma=1$ is stable under the evolution (14). We will now restrict our study to this totally efficient case and consider only pure state dynamics. We show then in Appendix C that Eq. (14) takes then the form of the two-dimensional PDMP Eq. (C3) for $(\theta_t^\gamma,\varphi_t^\gamma)$:

$$\begin{aligned}\dot\theta_t^\gamma&=\Big[-2k_{\gamma_1}\sin\big(\varphi_t^\gamma\big)-\frac{\gamma_1}{2}\sin\big(\theta_t^\gamma\big)\Big]+\big(\pi-\theta_t^\gamma\big)\dot{\tilde{\mathcal{N}}}_t^{1,\gamma},\\ \dot\varphi_t^\gamma&=-2k_{\gamma_1}\frac{\cos\big(\theta_t^\gamma\big)}{\sin\big(\theta_t^\gamma\big)}\cos\big(\varphi_t^\gamma\big)\end{aligned}\tag{17}$$

with

$$\mathbb{E}\big(d\tilde{\mathcal{N}}_t^{1,\gamma}\big|\theta_t^\gamma\big)=\gamma_1\left(\sin\frac{\theta_t^\gamma}{2}\right)^2dt,\quad d\tilde{\mathcal{N}}_t^{1,\gamma}d\tilde{\mathcal{N}}_t^{1,\gamma}=d\tilde{\mathcal{N}}_t^{1,\gamma}.$$

Note that the Poisson noise part effect is a resetting [58–61] in the south pole of the Bloch ball $\theta=\pi$ [see Eq. (8)].

It is clear from the second equation of Eq. (17) that the plane $\varphi_t=\frac{\pi}{2}$ is stable, and then by restricting the dynamics to this plane, we see that θ_t^γ is the one-dimensional PDMP given by

$$\dot\theta_t^\gamma=\left(-2k_{\gamma_1}-\frac{\gamma_1}{2}\sin\big(\theta_t^\gamma\big)\right)+\big(\pi-\theta_t^\gamma\big)\dot{\tilde{\mathcal{N}}}_t^{1,\gamma}.\tag{18}$$

This equation was first studied in [65] and later in [66] and will be the starting point of our analytical study in the collapse-unitary setup (see Sec. V A). Again, when $\gamma_1=0$, this is the usual equation for Rabi oscillations [75,76], i.e., $\theta_t^0=-2k_0t$, which implies for the density matrix (15)

$$\rho_t^0=\frac{1}{2}\begin{pmatrix}1+\cos(-2k_0t) & i\,\sin(2k_0t)\\ -i\,\sin(2k_0t) & 1-\cos(-2k_0t)\end{pmatrix}.\tag{19}$$

Note finally that [65,66] contains a different derivation of Eq. (18), by starting for a model of indirect measurement [22,24] with two-dimensional probes.

[2]This parametrization is quite unusual but it is convenient for our purpose.

In Fig. 1 we show plots of the trajectory of the process for different values of γ_1 and the choice $k_{\gamma_1}=\sqrt{\omega\gamma_1}$ (a negative sign will not change the results). This scaling with γ_1 is chosen in order to see the spikes (see Appendix D for justification).

B. Collapse-thermal setup: Measurement of thermal fluctuations

We choose here $H=0$, no extra measurement apart from N_1 and the thermal Lindbladian in a weak coupling form [77]

$$\begin{aligned}L^{th}[\rho]=&M_+\rho M_+^\dagger-\tfrac{1}{2}M_+^\dagger M_+\rho-\tfrac{1}{2}\rho M_+^\dagger M_+\\&+M_-\rho M_-^\dagger-\tfrac{1}{2}M_-^\dagger M_-\rho-\tfrac{1}{2}\rho M_-^\dagger M_-,\end{aligned}$$

with

$$M_+=\sqrt{W_{-,+}}\begin{pmatrix}0&1\\0&0\end{pmatrix},\quad M_-=\sqrt{W_{+,-}}\begin{pmatrix}0&0\\1&0\end{pmatrix},$$

where $W_{-,+}$, $W_{+,-}$ are positive coefficients characterizing the thermal bath. We use the parametrization given in Eq. (10). The components q_t^γ of the SME equation (1) evolve then autonomously as a one-dimensional PDMP defined by

$$\begin{aligned}\dot q_t^\gamma=&(W_{+,-}+W_{-,+})\left(\frac{W_{-,+}}{W_{+,-}+W_{-,+}}-q_t^\gamma\right)\\&-q_t^\gamma\big(\dot{\mathcal{N}}_t^{1,\gamma}-\gamma_1\eta_1\big(1-q_t^\gamma\big)\big),\end{aligned}\tag{20}$$

with

$$\mathbb{E}\big(d\mathcal{N}_t^{1,\gamma}\big|q_t^\gamma\big)=\gamma_1\eta_1\big(1-q_t^\gamma\big)dt,\quad d\mathcal{N}_t^{1,\gamma}d\mathcal{N}_t^{1,\gamma}=d\mathcal{N}_t^{1,\gamma}.$$

In Fig. 2 we show plots of the trajectory of the process for different values of γ_1.

C. Collapse-measurement setup: Competition between two measurements

We choose here $H=L^{th}=0$ and $p=2$ with two noncommuting reset measurement operators: the collapse-measurement operator $N_1=|-\rangle\langle-|$, with rate γ_1, and the damping-spontaneous emission operator N_2 defined by

$$N_2=\begin{pmatrix}0&1\\0&0\end{pmatrix}=|+\rangle\langle-|,\tag{21}$$

acting with rate γ_2.

Observe that N_2 does not commute with N_1, so QND property is broken. Note that not only is it nondiagonal in the basis $|+\rangle,|-\rangle$, the matrix N_2 is in fact not diagonal in any basis. This means that even ignoring the N_1 measurement, the measurement of N_2 does not satisfy the QND hypothesis and, therefore, is not by itself an *a priori* collapse dynamics. This is why we use the generic word "Measurement" in the title of this section.

Anyway, since N_2 is of rank one, the term $M_{N_2}[\rho_t^\gamma]\dot{\mathcal{N}}_t^{2,\gamma}$ is a resetting dynamics to $|+\rangle\langle+|$. This is because

$$\rho\to\rho+M_{N_2}[\rho]=\frac{N_2\rho N_2^\dagger}{\mathrm{Tr}(N_2\rho N_2^\dagger)}=|+\rangle\langle+|\,.\tag{22}$$

Hence, we have here a competition between a resetting dynamics to $|-\rangle\langle-|$ induced by N_1 and a resetting dynamics to $|+\rangle\langle+|$ induced by N_2. Note that in Sec. VI, we will discuss extension to more general choice of operator N_2.

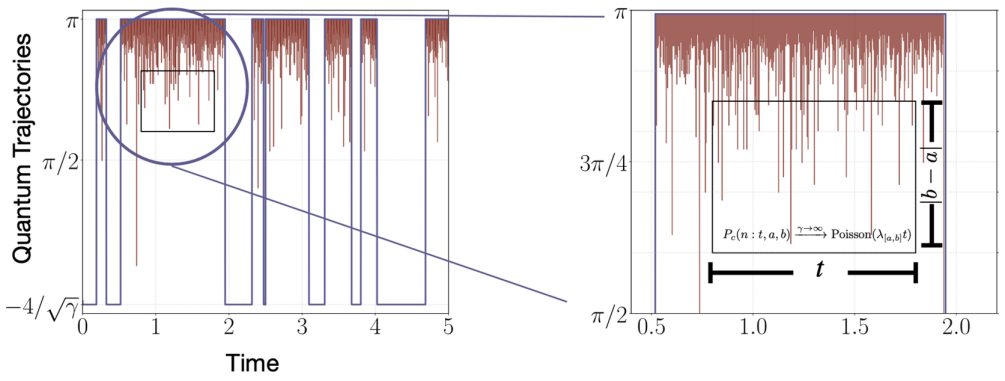

FIG. 4. Pictorial depiction of the construction of $P_c(n:t,a,b)$: the probability of observing n prespikes, given that there are no jumps in-between. Quantum trajectories are characterized by quantum jumps (shown in violet) and are accompanied by spikes (shown in brown). The spike statistics occurring between consecutive jumps within a black box of width $|b-a|$ and length t is the focus of this article. It is anticipated that at large measurement strength, these spike statistics follow a Poisson distribution.

As before we use the parametrization given in Eq. (10). The SME (1) becomes then autonomous for the diagonal [see Eq. (11) and Appendix B]

$$\begin{aligned}\dot{q}_t^\gamma &= -q_t^\gamma\big(\dot{\mathcal{N}}_t^{1,\gamma} - \gamma_1\eta_1(1-q_t^\gamma)\big)\\ &\quad + \gamma_2(1-q_t^\gamma) + (1-q_t^\gamma)\big(\dot{\mathcal{N}}_t^{2,\gamma} - \gamma_2\eta_2(1-q_t^\gamma)\big),\end{aligned} \tag{23}$$

with

$$\mathbb{E}\big(d\mathcal{N}_t^{k,\gamma}\big|q_t^\gamma\big) = \gamma_k\eta_k(1-q_t^\gamma)dt,\ d\mathcal{N}_t^{k,\gamma}d\mathcal{N}_t^{\ell,\gamma} = \delta_{k\ell}\,d\mathcal{N}_t^{k,\gamma}.$$

In Fig. 3, we show plots of the trajectory of the collapse-measurement setup for different values of γ_1.

IV. SUMMARY OF MAIN RESULTS IN THE PRECISE SETUP

From numerical simulations (see Figs. 1–3), we observe that, in the large-γ limit, a typical trajectory is composed of two parts. The first part is given by a pure jump Markov process with state space[3] $\{0,\pi\}$ (in the collapse-unitary setup) or $\{0,1\}$ (in the collapse-thermal and collapse-measurement setups), corresponding to quantum jumps.

The second part is a decoration of this trajectory by a large number of one-sided vertical lines connecting π in the collapse-unitary setup (respectively 0 in the collapse-thermal and collapse-measurement setups) to random values in $(0,\pi)$ [respectively (0,1) in the collapse-thermal and collapse-measurement setups] at random times. These vertical lines correspond in fact to the deterministic trajectories (we call them prespikes) during successive clicks in the strong measurement limit. Our main goal now is to describe the statistics of the clicks in the strong measurement regime. Since the spikes originate only on the part of the quantum jump trajectory equal to π for the collapse-unitary case and 0 for the other two cases, we will focus on, respectively, these precise initial conditions.

[3]The fact that the state space is $\{0,\pi\}$ and not $\{0,1\}$ is due to the change of variable done in Eq. (15).

As seen in Figs. 1–3, for any finite γ, the prespikes have a specific structure consisting of a deterministic flow and a sudden reset to a particular state. In the special limit $\gamma\to\infty$, the prespikes become infinitely thin and occur with an infinite density (in time), and have a distribution of heights. Hence, we have a clear picture of how spikes emerge from prespikes. To characterize the statistic of spikes precisely, we define a spike to be localized at time t, if its tip ends at a spatial point x. We then ask for the number of spikes observed in a two-dimensional space-time box of width $(0,t)$ in time and (a,b) in space.

The probability of observing n prespikes, conditioned on no jumps (i.e., no prespikes whose tips extend to the opposite end, see Fig. 4) occurring during this time window, will be denoted by $P_c(n:t,a,b)$. To be more precise, as explained above, we focus only on initial conditions for which we can observe prespikes before a quantum jump, i.e., π in the collapse-unitary setup and 0 in the other cases. Hence, we describe the nontrivial spike statistics only during the (random) period of time in which the investigated process starts from a pointer state with spikes and does not jump to a new pointer state (without spikes) during this time period. By Markov property our analysis is in fact valid for any period of time where we really have spikes.

One of our main results of this paper is the proof, in the limit of large γ, of the Poisson distribution:

$$\begin{aligned}\lim_{\gamma\to\infty} P_c(n:t,a,b) &= \frac{(\lambda_{[a,b]}t)^n}{n!}\ \exp(-\lambda_{[a,b]}t)\\ \text{where } \lambda_{[a,b]} &= \int_a^b dx\, I(x)\,,\end{aligned} \tag{24}$$

and the intensity for the three cases is, respectively, given by

$$\begin{aligned}I(x) &= \frac{4\omega\,\sin(x/2)}{\cos^3(x/2)} \quad \text{collapse-unitary}\\ &= \frac{W_{-,+}}{x^2} \quad \text{collapse-thermal}\\ &= \frac{\gamma_2(1-\eta_2)}{x^2} \quad \text{collapse-measurement.}\end{aligned} \tag{25}$$

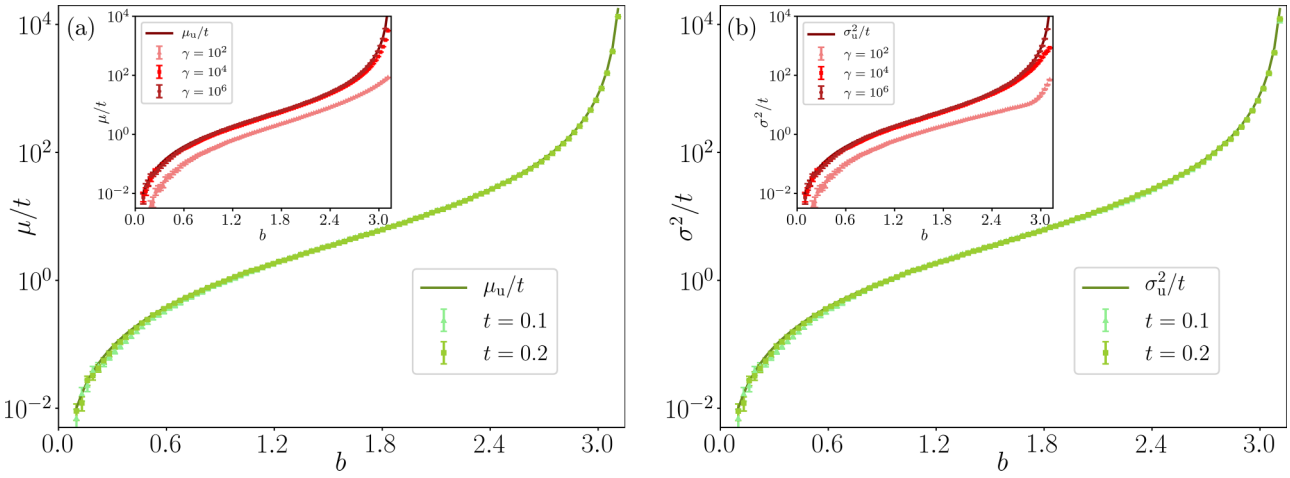

FIG. 5. Collapse-unitary case: (a) mean and (b) variance of the distribution (conditioned on no jumps) of the number of spikes (from $\theta_t = \pi$) per unit time in a space-time box $(0, b) \times (0, t)$ plotted against the box edge b for $\gamma = 10^6$. The data points were obtained for $\omega = 1$ by averaging over 10^4 realizations. μ_u and σ^2_u are the mean and variance, respectively, of the theoretically predicted Poisson process in Eq. (24). The data in the insets, plotted for a fixed time $t = 0.1$, converge to μ_u/t and σ^2_u/t at large γ.

Some comments follow:

(i) In Figs. 5–7 we show a comparison of the above analytic forms of the three processes with computations of the mean and variance of the spike statistics obtained from numerical simulations. The Poisson property is illustrated by the overlap of the empirical mean and the empirical variance. In all cases we see excellent agreement of the numerics with the analytic predictions.

(ii) The first result, in the collapse-unitary setup, is proved only for the fully efficient case ($\eta_1 = 1$) while the latter two are valid for any nonvanishing efficiency ($0 < \eta_1 \leqslant 1$). Anyway, numerical simulation of the inefficient case ($0 < \eta_1 < 1$) in the collapse-unitary setup [i.e., equation Eq. (14)] shows that the spikes exist anyway in the nonautonomous q process (see Fig. 8).

(iii) By a change of variable $q = (1 + \cos x)/2$ for the first case, all three intensities acquire the same universal form. This change of variable is in fact natural since it corresponds to returning to the representation of the qubit in Eq. (10) with the inverse of the change of variable given by Eq. (15). Interestingly, the spikes statistics above are similar to the spike statistics obtained in [52–54,56], in the case where the noise $\mathcal{N}$ is not Poissonian, but Gaussian.

(iv) In the collapse-measurement setup, for a perfect measurement efficiency of N_2 (i.e., $\eta_2 = 1$), the spikes disappear completely, indicating a complex interplay of measurement of two noncommuting observables in non-QND measurement.

(v) In these three cases, the jump transition rates of the jump process can be computed explicitly. In the collapse-unitary setup, the jumps between the two pointer states occur

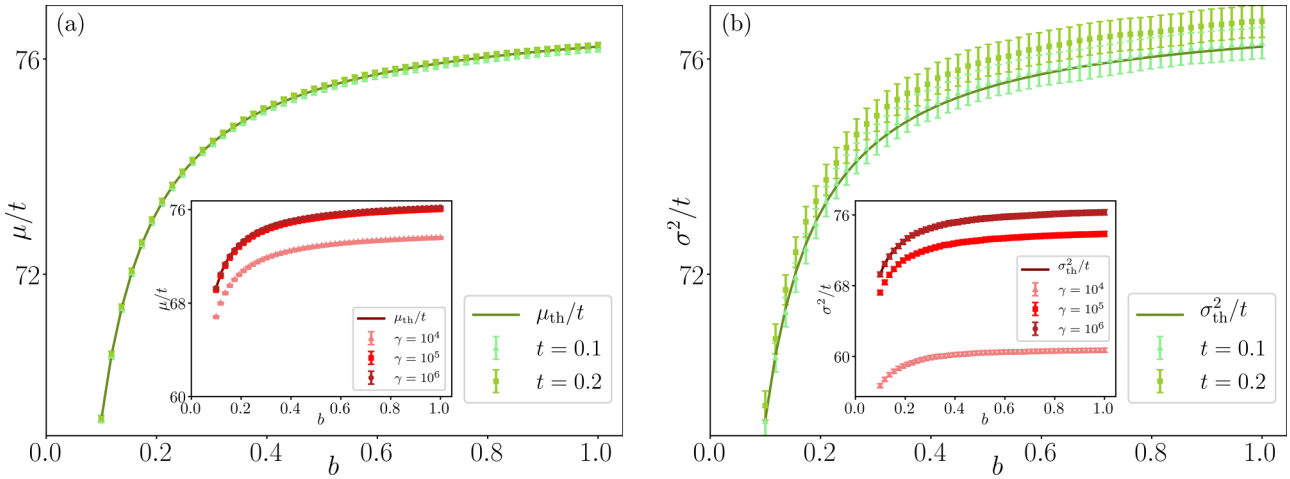

FIG. 6. Collapse-thermal case: (a) mean and (b) variance of the distribution (conditioned on no jumps) of the number of spikes (from $q_t = 0$) per unit time in a space-time box $(0.01, b) \times (0, t)$ plotted against the box edge b for $\gamma = 10^6$. The data points were obtained for the parameters $W_{-,+} = 0.77$, $W_{+,-} = 0.23$ by averaging over 10^5 realizations. μ_{th} and σ^2_{th} are the mean and variance, respectively, of the theoretically predicted Poisson process in Eq. (24). The data in the insets, plotted for a fixed time $t = 0.1$, converge to μ_{th}/t and σ^2_{th}/t at large γ.

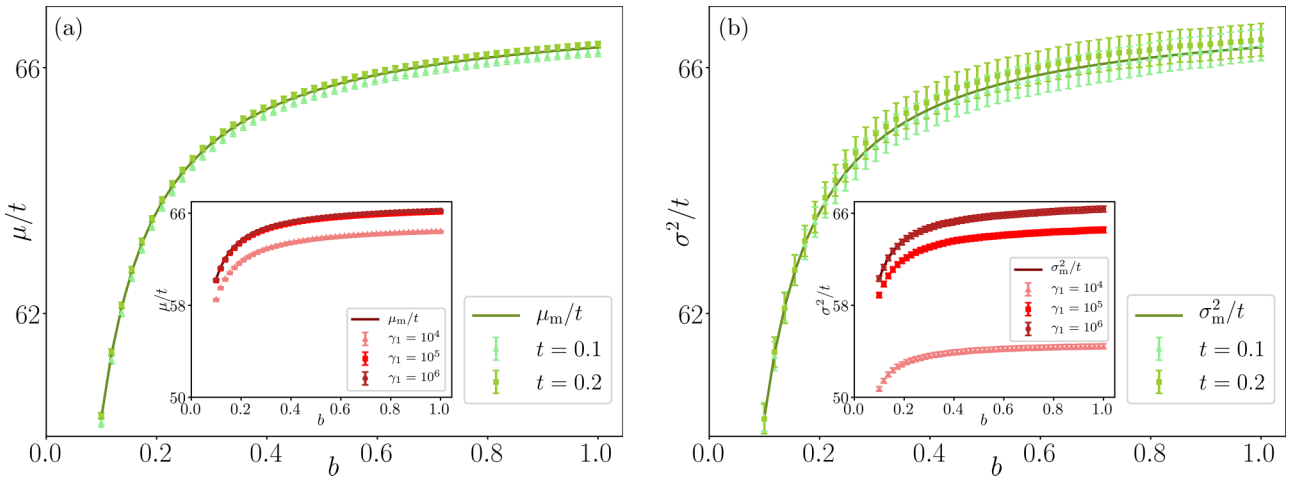

FIG. 7. Collapse-measurement case: (a) mean and (b) variance of the distribution (conditioned on no jumps) of the number of spikes (from $q_t = 0$) per unit time in a space-time box $(0.01, b) \times (0, t)$ plotted against the box edge b for $\gamma_1 = 10^6$. The data points were obtained for the parameters $\gamma_2 = 1$ and $\eta_1 = \eta_2 = 0.33$ by averaging over 10^5 realizations. μ_m and σ^2_m are the mean and variance, respectively, of the theoretically predicted Poisson process in Eq. (24). The data in the insets, plotted for a fixed time $t = 0.1$, converge to μ_m/t and σ^2_m/t at large γ_1.

with rate 4ω while in the collapse-thermal setup, the jumps between the states occur with rates $W_{-,+}$ and $W_{+,-}$ respectively, and in the collapse-measurement setup, only transitions are one sided with rate γ_2 (parameters are specified in Sec. III).

V. MATHEMATICAL DERIVATIONS

A. Study in the collapse-unitary setup

To simplify notation, we denote γ_1 by γ and $\tilde{\mathcal{N}}^{1,\gamma}$ by $\mathcal{N}$, θ^γ by θ. We also choose $k_\gamma = \sqrt{\omega\gamma}$ in order to get quantum spikes in the large-γ limit (see Appendix D for justification). The dynamics is then specified by the following stochastic evolution equation [see Eq. (18)]:

$$d\theta_t = \Omega(\theta_t)dt + (\pi - \theta_t)d\mathcal{N}_t, \tag{26}$$

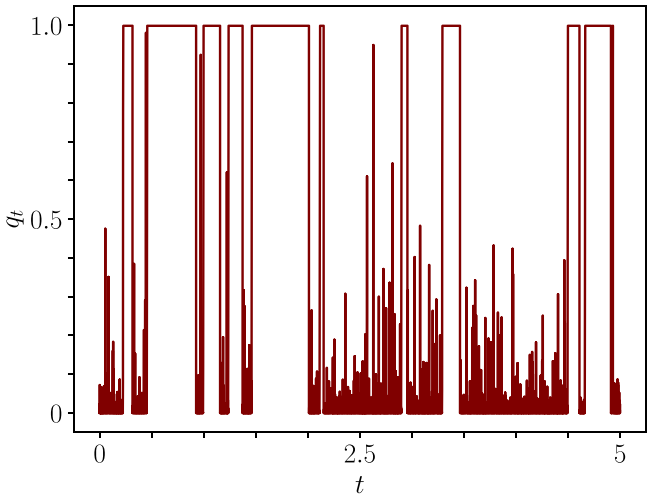

FIG. 8. Typical trajectories for collapse-unitary setup for inefficient measurements, for the parameters $\eta_1 = 0.33$, $\gamma = 10^4$, and $\omega = 1$. Similar to the collapse-thermal and collapse-measurement cases, the jumps between $q_t = 0$ and 1 are interspersed with spikes from $q_t = 0$ in the strong measurement limit.

where the drift term $\Omega := \Omega^\gamma$ and the Poissonian noise $\mathcal{N}$ satisfy

$$\Omega(\theta) = -2\sqrt{\omega\gamma}\left[1 + \sqrt{\frac{\gamma}{16\omega}}\sin\theta\right], \tag{27}$$

$$\mathbb{E}[d\mathcal{N}_t|\theta_t] = \alpha(\theta_t)\,dt := \gamma\,\sin^2\frac{\theta_t}{2}\,dt. \tag{28}$$

Hence the dynamics evolves deterministically in $[\theta^* = -\sin^{-1}(4\sqrt{\omega/\gamma}), \pi]$ but at some random times prescribed by $\mathcal{N}$, the angle is resetting to the value π, i.e., a "click" occurs. Rarely, during the deterministic evolution, no resetting occurs and the trajectory is able to reach θ^* and is stuck around θ^* for a random time until a new resetting to π occurs. In the large-γ limit, as $\theta^* \to 0$, we say then that we have a jump from π to 0 and afterwards a jump (instantaneous) from 0 to π.

With the notations of [66], the situation considered here corresponds then to the special case $\gamma_0 = \sqrt{\omega\gamma}$, or equivalently $\lambda = \gamma/(4\gamma_0) = \sqrt{\frac{\gamma}{16\omega}}$. We recall that we are interested in the strong measurement regime $\gamma \to \infty$, not investigated in [66]. Hence, the angle $\hat{\theta}_t$, evolving according to the deterministic equation

$$d\hat{\theta}_t = \Omega(\hat{\theta}_t)\,dt, \tag{29}$$

is confined to the range $[-\sin^{-1}(1/\lambda), \pi] \approx (-4\sqrt{\omega/\gamma}, \pi)$, the last approximation being valid since γ is large. In particular, for $t \geqslant 0$, we have the exact solution [66]

$$\tan\left(\frac{\hat{\theta}_t(0|\pi)}{2}\right) = -\frac{\sinh(\beta\sqrt{\omega\gamma}\,t - \phi)}{\sinh(\beta\sqrt{\omega\gamma}\,t)}, \tag{30}$$

where

$$\beta = \sqrt{\frac{\gamma}{16\omega} - 1} = \sinh(\phi)\,. \tag{31}$$

Let τ be the time taken by a deterministic trajectory $\hat{\theta}$ to evolve from $\hat{\theta}_0 = \pi$ to $\hat{\theta}_\tau = 0$. From Eq. (30), we note $\tau = \phi/(\beta\sqrt{\omega\gamma})$. For $\gamma \gg 1$, $\tau \approx 2\log\gamma/\gamma$. If $c \in (0, \pi)$, let us also denote the time for the deterministic dynamics to reach

c when starting from π by τ_c. A straightforward inversion of Eq. (30) yields

$$\tau_c = \frac{1}{2\beta\sqrt{\omega\gamma}} \log\left[1 + \frac{2\beta}{\tan(c/2) + e^{-\phi}}\right]. \tag{32}$$

Given that the initial state is θ_0, we consider the probability $p_0^t(t_1, t_2, \ldots, t_n|\theta_0)$ of observing no jumps and a sequence of n clicks occurring exactly at times $t_1 < t_2 < \ldots t_n$ within the time interval $(0, t)$. The no-jump condition is enforced by the inequality $\tau \geqslant t_j - t_{j-1}$ for any $j \leqslant n$. The quantum trajectory is deterministic between the clicks and the sequence $\{\theta_0, \theta_{t_1}, \pi, \theta_{t_2}, \pi, \ldots, \theta_{t_n}, \pi, \theta_t\}$ determines the quantum trajectory. The evolution from $\theta_0 \to \theta_{t_1}$, $\pi \to \theta_{t_i}$ (for $i = 2, \ldots, n$) and $\pi \to \theta_t$ is given by the deterministic flow in Eq. (29).

Let us define $\mu(\Delta t|\theta_i)$ as the probability to not have a click during the time interval Δt for the initial condition $\theta = \theta_i$. This is given by

$$\mu(\Delta t|\theta_i) = e^{-\int_0^{\Delta t} ds\, \alpha[\hat{\theta}_s(0|\theta_i)]} = \frac{\Omega(\theta_i)}{\Omega[\hat{\theta}_{\Delta t}(0|\theta_i)]} e^{-\frac{\gamma \Delta t}{2}}. \tag{33}$$

Then we have

$$\begin{aligned} &p_0^t(t_1, t_2, \ldots, t_n|\hat{\theta}_0) \\ &\quad = \mu(t_1|\theta_0)\alpha(\hat{\theta}_{t_1}) \prod_{i=2}^{n} \left[\mu(t_i - t_{i-1}|\pi)\alpha\big(\hat{\theta}_{t_i - t_{i-1}}(0|\pi)\big)\right] \\ &\qquad \times \mu(t - t_n|\pi). \end{aligned} \tag{34}$$

Using the explicit solution in Eq. (30) and after some algebra we get

$$\begin{aligned} \mu(t|\pi)\,\alpha[\hat{\theta}_t(0|\pi)] &= \frac{\gamma\, \sinh^2(\beta\sqrt{\omega\gamma}t - \phi)}{\beta^2}, \\ \mu(t|\pi) &= \frac{\sinh^2(\beta\sqrt{\omega\gamma}t) + \sinh^2(\beta\sqrt{\omega\gamma}t - \phi)}{\beta^2}. \end{aligned} \tag{35}$$

The joint probability $P_j(n : t, a, b)$ to observe exactly n prespikes in the time interval $[0, t]$ and in the space interval $[a, b]$ (where $0 < a < b < \pi$), starting from π, and such that no jumps occur in the time interval $[0, t]$, is given by

$$\begin{aligned} &P_j(n : t, a, b) \\ &\quad = \sum_{m=0}^{\infty} \frac{(n+m)!}{n!m!} \prod_{i=1}^{n+m} \int_0^{t_{i+1}} dt_i\, p_0^t(t_1, t_2, \ldots, t_{n+m}|\pi) \\ &\qquad \times \prod_{j=1}^{m} \{\Theta[\tau_b - (t_j - t_{j-1})] + \Theta[(t_j - t_{j-1}) - \tau_a]\} \\ &\qquad \times \prod_{j=1}^{n} \Theta[(t_j - t_{j-1}) - \tau_b]\, \Theta[\tau_a - (t_j - t_{j-1})] \\ &\qquad \times \prod_{j=1}^{n+m} \Theta[\tau - (t_j - t_{j-1})]\, \Theta[\tau - (t - t_{n+m})], \end{aligned} \tag{36}$$

where we have defined $t_{n+m+1} = t$ and Θ is the Heaviside function. Taking time-Laplace transform $\hat{P}_j(n : \sigma, a, b) = \int_0^\infty dt\, e^{-\sigma t} P_j(n : t, a, b)$ gives

$$\hat{P}_j(n : \sigma, a, b) = \sum_{m=0}^{\infty} \frac{(n+m)!}{n!m!} C^m(\sigma) D^n(\sigma) E(\sigma), \tag{37}$$

where

$$\begin{aligned} C(\sigma) &= \int_0^\infty dt\, \mu(t|\pi)\,\alpha[\hat{\theta}_t(0|\pi)]\,[\Theta(\tau_b - t) + \Theta(t - \tau_a)] \\ &\quad \times \Theta(\tau - t)\, e^{-\sigma t}, \\ D(\sigma) &= \int_0^\infty dt\, \mu(t|\pi)\,\alpha[\hat{\theta}_t(0|\pi)]\,\Theta(\tau_a - t)\Theta(t - \tau_b) e^{-\sigma t}, \\ E(\sigma) &= \int_0^\infty dt\, \mu(t|\pi)\,\Theta(\tau - t)\, e^{-\sigma t}. \end{aligned} \tag{38}$$

Performing the summation, we get

$$\hat{P}_j(n : \sigma, a, b) = \frac{D^n(\sigma) E(\sigma)}{[1 - C(\sigma)]^{1+n}}. \tag{39}$$

Writing the generating function $(0 \leqslant s \leqslant 1)$

$$Z(s : \sigma, a, b) = \sum_{n=0}^{\infty} s^n \hat{P}_j(n : \sigma, a, b), \tag{40}$$

we find the exact formula

$$Z(s : \sigma, a, b) = \frac{E(\sigma)}{1 - C(\sigma) - sD(\sigma)}. \tag{41}$$

Thanks to the explicit expressions (35), the functions $C(\sigma)$, $D(\sigma)$, and $E(\sigma)$ can be computed explicitly and their asymptotic behavior for large γ can be obtained (see Appendix E for details). It follows that for any $s \in [0, 1]$ fixed we have in the large-γ limit that

$$\begin{aligned} &Z(s : \sigma, a, b) \\ &\quad \approx \frac{1}{\sigma + 4\omega + 4\omega(1 - s)[\tan^2(b/2) - \tan^2(a/2)]}. \end{aligned} \tag{42}$$

The probability $S(t)$ of no jump occurring from π to 0 in the time interval $(0, t)$ is obtained by taking $s = 1$ in the generating function in Eq. (42), which yields $S(t) = e^{-4\omega t}$. Since $1 - S(t)$ is the cumulative distribution function of the distribution of time of first passage from π to 0, this implies that the first time to reach 0 is exponentially distributed with a mean equal to $1/(4\omega)$. The probability $P_c(n : t, a, b)$ to observe exactly n prespikes in the time interval $[0, t] \times [a, b]$, *given* that no jump occurs in the time interval $[0, t]$, can be obtained by

$$P_c(n : t, a, b) = \frac{P_j(n : t, a, b)}{S(t)},$$

which is given by the Poisson distribution in the large-γ limit [as announced in Eq. (24)]

$$\frac{(\lambda_{[a,b]} t)^n e^{-\lambda_{[a,b]} t}}{n!}, \quad \text{where } \lambda_{[a,b]} = \int_a^b dx\, \frac{4\omega \sin(x/2)}{\cos^3(x/2)}. \tag{43}$$

Moreover, by using Eqs. (33) and (30) we have that the probability to have no resetting to π by starting from 0 in a

time interval of length Δt is given by

$$\mu(\Delta t|0) = \frac{-2\sqrt{\omega\gamma}\,e^{-\frac{\gamma\Delta t}{2}}}{\Omega\Big[-2\tan^{-1}\Big(\frac{\sinh(\beta\sqrt{\omega\gamma}\Delta t)}{\sinh(\beta\sqrt{\omega\gamma}\Delta t+\phi)}\Big)\Big]}. \tag{44}$$

By performing the expansion in γ we get that

$$\mu(\Delta t|0) \approx \exp(-4\omega\Delta t), \tag{45}$$

so that the time to be resetting to π when starting from 0 is also exponentially distributed with mean $1/(4\omega)$.

B. Study in the collapse-thermal setup

To simplify notation, we denote γ_1 by γ and $\mathcal{N}^{1,\gamma}$ by $\mathcal{N}$, q_t^γ by q_t. Equation (20) can then be rewritten as

$$dq_t = \Omega(q_t)dt - q_t\, d\mathcal{N}_t, \tag{46}$$

where the quadratic drift term Ω and the rate function α of $\mathcal{N}_t$ are given by

$$\Omega(q) = W_{-,+} - q(W_{+,-} + W_{-,+} - \gamma\eta) - \gamma\eta q^2,$$
$$\mathbb{E}[d\mathcal{N}_t|q_t] = \alpha(q_t)\,dt = \gamma\eta(1-q_t)\,dt. \tag{47}$$

The roots of $\Omega(q)$ are the fixed points of the no-click deterministic dynamics, given by

$$q_\pm = \frac{\gamma\eta - W_{+,-} - W_{-,+} \pm \sqrt{(W_{+,-} + W_{-,+} - \gamma\eta)^2 + 4W_{-,+}\gamma\eta}}{2\gamma\eta},$$

which are always real and distinct. Note that $q_- < 0 < q_+$, provided all the parameters are not identically zero. For an initial condition $q_0 < q_+$, the stochastic dynamics is confined to $[0, q_+)$ for $\gamma \gg 1$.

The solution of the deterministic equation $d\hat{q}_t = \Omega(\hat{q}_t)dt$ starting from q_0 is given by

$$\hat{q}_t(q_0) = \frac{q_+(q_0-q_-) + q_-(q_+-q_0)e^{-\gamma\eta(q_+-q_-)t}}{(q_0-q_-) + (q_+-q_0)e^{-\gamma\eta(q_+-q_-)t}}. \tag{48}$$

For $c \in [0,1]$, let τ_c be the time taken to evolve from $q_0 = 0$ to $q = c$. A straightforward inversion of Eq. (48) shows that

$$\tau_c = \frac{1}{\eta\gamma(q_+-q_-)}\log\left|\frac{(c-q_-)q_+}{q_-(q_+-c)}\right|, \tag{49}$$

and let τ be the time taken by a deterministic trajectory to evolve from $q = 0$ to $1-\epsilon$. For $\gamma \gg 1$,

$$\tau \sim \frac{1}{\gamma\eta}\log\left|\frac{\gamma^2\eta^2(1-\epsilon)}{W_{+,-}W_{-,+} + \epsilon(\gamma^2\eta^2 - W_{+,-}\gamma\eta)}\right|.$$

Similar to the collapse-unitary case, we explicitly obtain the functions

$$\mu(t|q_0) = e^{-\int_0^t ds\,\alpha[\hat{q}_s(q_0)]}$$
$$= \frac{(q_0-q_-)e^{-\gamma\eta(1-q_+)t} + (q_+-q_0)e^{-\gamma\eta(1-q_-)t}}{q_+-q_-},$$
$$\mu(t|q_0)\alpha[q_t(q_0)]$$
$$= \tfrac{\gamma\eta}{q_+-q_-}[(q_0-q_-)(1-q_+)e^{-\gamma\eta(1-q_+)t}$$
$$+ (q_+-q_0)(1-q_-)e^{-\gamma\eta(1-q_-)t}], \tag{50}$$

which we plug into the Eq. (38) to explicitly obtain the functions $C(\sigma)$, $D(\sigma)$, and $E(\sigma)$ and obtain their asymptotic behavior for large γ (see Appendix E for details).

Consider the probability $P_j(n:t,a,b)$ to observe exactly n prespikes in the time interval $[0,t]$ and in the space interval $[a,b]$ (where $0 < a < b < 1$), and that no jump occurs in the time interval $[0,t]$, starting from 0. The corresponding generating function in the Laplace domain $Z(s:\sigma,a,b)$, defined in Eq. (40), can be obtained by plugging $C(\sigma)$, $D(\sigma)$, and $E(\sigma)$ into Eq. (41). It follows that for any $s \in [0,1]$ fixed we have in the large-γ limit that

$$\lim_{\gamma\to\infty} Z(s:\sigma,a,b) = \frac{1}{\sigma + W_{-,+} + W_{-,+}(1-s)\big(\frac{1}{a}-\frac{1}{b}\big)}. \tag{51}$$

The probability $S(t)$ of no jump occurring from 0 to 1 in the time interval $(0,t)$ is obtained by taking $s = 1$ in the generating function in Eq. (42), which yields $S(t) = e^{-W_{-,+}t}$. This implies that the first time to reach 1 starting from 0 is exponentially distributed with a mean equal to $1/W_{-,+}$. The probability $P_c(n:t,a,b)$ to observe exactly n spikes in the time interval $[0,t]\times[a,b]$, *given* that no jump occurs in the time interval $[0,t]$, can be obtained by

$$P_c(n:t,a,b) = \frac{P_j(n:t,a,b)}{S(t)},$$

which is given by the Poisson distribution in the large-γ limit [as announced in Eq. (24)]

$$\frac{(\lambda_{[a,b]}t)^n e^{-\lambda_{[a,b]}t}}{n!}, \quad \text{where } \lambda_{[a,b]} = \int_a^b dx\,\frac{W_{-,+}}{x^2}. \tag{52}$$

Moreover, similar to the collapse-unitary setup, we have that the probability to have no resetting to 0 by starting from 1 in a time interval of length Δt is given for large γ by

$$\mu(\Delta t|1) \approx \exp(-W_{+,-}\Delta t), \tag{53}$$

so that the time to be resetting to 0 when starting from 1 is exponentially distributed with mean $1/W_{+,-}$.

C. Study in the collapse-measurement setup

To simplify notation, we denote $\mathcal{N}^{1,\gamma_1}$ by $\mathcal{N}^1$, $\mathcal{N}^{2,\gamma_2}$ by $\mathcal{N}^2$, and q_t^γ by q_t. Equation (23) can then be rewritten as

$$dq_t = \Omega(q_t)dt - q_t\, d\mathcal{N}_t^1 + (1-q_t)\, d\mathcal{N}_t^2, \tag{54}$$

where the quadratic drift term $\Omega := \Omega^{\gamma_1,\gamma_2}$ and the rate functions α of $\mathcal{N}_t^1$ and $\tilde{\alpha}$ of $\mathcal{N}_t^2$ are given by

$$\Omega(q) = (\gamma_2 + q\gamma_1\eta_1)(1-q) - \gamma_2\eta_2(1-q)^2,$$
$$\mathbb{E}\big(d\mathcal{N}_t^1\big|q_t\big) = \alpha(q_t)\,dt = \gamma_1\eta_1(1-q_t)dt,$$
$$\mathbb{E}\big(d\mathcal{N}_t^2\big|q_t\big) = \tilde{\alpha}(q_t)\,dt = \gamma_2\eta_2(1-q_t)dt. \tag{55}$$

The roots of $\Omega(q)$ are the fixed points of the no-click dynamics, given by

$$q_- = \frac{\gamma_2(\eta_2-1)}{\gamma_2\eta_2 + \gamma_1\eta_1}, \quad q_+ = 1. \tag{56}$$

Note that $q_- < 0$ (provided N_2 is not measured with unit efficiency).

The solution of the deterministic equation $d\hat{q}_t = \Omega(\hat{q}_t)dt$, starting from q_0 at time $t = 0$, is given by

$$\hat{q}_t(q_0) = \frac{(q_0 - q_-) + q_-(1 - q_0)e^{-(\gamma_1\eta_1 + \gamma_2\eta_2)(1-q_-)t}}{(q_0 - q_-) + (1 - q_0)e^{-(\gamma_1\eta_1 + \gamma_2\eta_2)(1-q_-)t}}. \quad (57)$$

For $c \in [0, 1]$, let τ_c be the time taken to evolve from $q_0 = 0$ to $q = c$. A straightforward inversion of Eq. (57) shows that

$$\tau_c = \frac{1}{(\eta_1\gamma_1 + \eta_2\gamma_2)(1 - q_-)} \log\left|\frac{(c - q_-)}{q_-(1 - c)}\right|. \quad (58)$$

Let τ be the time taken by a deterministic trajectory to evolve from $q = 0$ to $1 - \epsilon$. For $\gamma_1 \gg 1$,

$$\tau \sim \frac{1}{\gamma_1\eta_1} \log\left|\frac{\gamma_1\eta_1(1 - \epsilon)}{\epsilon\gamma_2(\eta_2 - 1)}\right|.$$

Similar to the collapse-unitary and collapse-thermal cases, we explicitly obtain the functions

$$\begin{aligned}\mu(t|q_0) &= e^{-\int_0^t ds(\alpha[\hat{q}_s(q_0)] + \tilde{\alpha}[\hat{q}_s(q_0)])} \\ &= \frac{(q_0 - q_-) + (1 - q_0)e^{-(\gamma_1\eta_1 + \gamma_2\eta_2)(1-q_-)t}}{1 - q_-}, \\ \mu(t|q_0)&\alpha[\hat{q}_t(q_0)] \\ &= \gamma_1\eta_1(1 - q_0)e^{-(\gamma_1\eta_1 + \gamma_2\eta_2)(1-q_-)t}, \end{aligned} \quad (59)$$

which we plug into Eq. (38) to explicitly obtain the functions $C(\sigma)$, $D(\sigma)$, and $E(\sigma)$ and obtain their asymptotic behavior for large γ (see Appendix E for details).

Consider the probability $P_j(n : t, a, b)$ to observe exactly n prespikes in the time interval $[0, t]$ and in the space interval $[a, b]$ (where $0 < a < b < 1$), and that no jump occurs in the time interval $[0, t]$, starting from 0. The corresponding generating function in the Laplace domain $Z(s : \sigma, a, b)$, defined in Eq. (40), can be obtained by plugging $C(\sigma)$, $D(\sigma)$, and $E(\sigma)$ into Eq. (41). It follows that for any $s \in [0, 1]$ fixed we have in the large-γ_1 limit (for γ_2 fixed)

$$\lim_{\gamma_1\to\infty} Z(s : \sigma, a, b) = \frac{1}{\sigma + \gamma_2 + (1 - s)\gamma_2(1 - \eta_2)\left(\frac{1}{a} - \frac{1}{b}\right)}. \quad (60)$$

The probability $S(t)$ of no jump occurring from 0 to 1 in the time interval $(0, t)$ is obtained by taking $s = 1$ in the generating function in Eq. (42), which yields $S(t) = e^{-\gamma_2 t}$. This implies that the first time to reach 1 starting from 0 is exponentially distributed with a mean equal to $1/\gamma_2$ and that the statistics of the spikes given the no-jump condition is given by the Poisson distribution in the large-γ_1 limit [as announced in Eq. (24)]

$$\frac{(\lambda_{[a,b]}t)^n e^{-\lambda_{[a,b]}t}}{n!}, \quad \text{where } \lambda_{[a,b]} = \int_a^b dx\, \frac{\gamma_2(1 - \eta_2)}{x^2}. \quad (61)$$

Note that, in this setup, the probability to have resetting to 0 by starting from 1 vanishes and the flow term out of 1 also vanishes. The mean time of first passage from 0 to 1 is γ_2^{-1} and, hence, spikes are typically not observed for $t \gg \gamma_2^{-1}$.

VI. GENERALIZATION: A GENERAL PERSPECTIVE ON SPIKES IN 1D PDMP

Our interest in spikes processes was motivated by quantum physics and its analytical description was limited by various technicalities (see the discussion below). But we may enlarge the discussion to cover other physical situations of interest.

To this end, let us consider a piecewise one-dimensional Markov process $(q_t^\gamma)_{t\geqslant 0}$ evolving according to the stochastic differential equation (SDE)

$$\dot{q}_t^\gamma = F\left(q_t^\gamma\right) + G\left(q_t^\gamma\right)\left(\dot{\mathcal{N}}_t^\gamma - \gamma H\left(q_t^\gamma\right)\right), \quad (62)$$

where $\mathcal{N}^\gamma$ is a Poisson process satisfying

$$\mathbb{E}\left(d\mathcal{N}_t^\gamma \middle| q_t^\gamma\right) = \gamma H\left(q_t^\gamma\right)dt, \quad d\mathcal{N}_t^\gamma\, d\mathcal{N}_t^\gamma = d\mathcal{N}_t^\gamma.$$

We assume that $G(q) > 0$ if $q \in]0, 1[$ and that

$$G(0)H(0) = 0 = G(1)H(1), \quad F(0) \geqslant 0, \quad F(1) \leqslant 0, \quad (63)$$

so that the process q^γ takes values in [0,1]. We conjecture that the graph $\{(t, q_t^\gamma)\,;\, t \geqslant 0\}$ of the process q^γ converges as $\gamma \to \infty$ to the random time-space "spike" graph $\mathbb{Q}$, which can be described as follows.

Let $(\bar{q}_t)_{t\geqslant 0}$ be the continuous pure jump Markov process on $\{0, 1\}$ with rate $F(0)$ [respectively $F(1)$] to jump from 0 to 1 (respectively from 1 to 0). The process $\bar{q}$ can be seen as the first rough description of q^γ for large γ, but it misses a more refined structure of the limit of q^γ.

"Decorate" then the trajectory $\bar{q}$ with spikes, which are vertical intervals (in space) included in [0,1], distributed as[4]

$$\mathbb{Q}_t = \begin{cases} [0, M_t], & \text{if } \bar{q}_{t-} = \bar{q}_t = 0 \\ [M_t, 1], & \text{if } \bar{q}_{t-} = \bar{q}_t = 1 \\ [0, 1], & \text{if } \bar{q}_{t-} \neq \bar{q}_t, \end{cases} \quad (64)$$

where, given the trajectory $\bar{q}$, $(t, M_t)_{t\geqslant 0}$ is the time-space Poisson process on $[0, \infty) \times [0, 1]$.

More precicely, the spikes from 0 to 1 have intensity $|F(0)|\mathbf{1}_{H(0)\neq 0}\, \frac{dt\, dx}{x^2}\, \mathbf{1}_{x\in[0,1]}$ and the spikes from 1 to 0 have intensity $|F(1)|\mathbf{1}_{H(1)\neq 0}\, \frac{dt\, dx}{(1-x)^2}\, \mathbf{1}_{x\in[0,1]}$ (See Fig. 9).

More explicitly, let $P_c[n : (s, t), a, b]$ be the probability of observing n tips of prespikes belonging to (a, b), conditioned on no jumps occurring during the time window (s, t). Its large-γ limit corresponds precisely to a Poisson distribution limit with parameter $\lambda^{\bar{q}}_{[a,b]}(t - s)$,

$$\text{i.e.,} \quad \lim_{\gamma\to\infty} P_c[n : (s, t), a, b] = \frac{(t - s)^n}{n!} e^{-\lambda^{\bar{q}}_{[a,b]}(t-s)}, \quad (65)$$

with the intensity parameter given by

$$\lambda^{\bar{q}}_{[a,b]} = \begin{cases} \int_a^b dx \frac{|F(0)|\,\mathbf{1}_{H(0)\neq 0}}{x^2} & \text{if} \quad \bar{q}\,\big|_{[s,t]} = 0, \\ \int_a^b dx \frac{|F(1)|\,\mathbf{1}_{H(1)\neq 0}}{(1-x)^2} & \text{if} \quad \bar{q}\,\big|_{[s,t]} = 1. \end{cases}$$

[4]Here $\bar{q}_{t-} =$, $\bar{q}_{t-\varepsilon}$ is the left limit of $\bar{q}$ at time t. By convention we assume that the process $\bar{q}_t$ has continuous from the right trajectories.

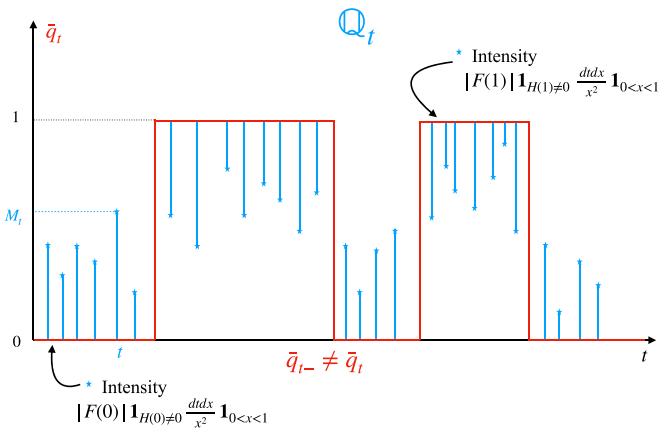

FIG. 9. The spike process $\mathbb{Q}_t$. The value M_t is the length of the spike at time t. The condition $\bar{q}_{t-} = \bar{q}_t = 0$ (respectively $\bar{q}_{t-} = \bar{q}_t = 1$) corresponds to the case where the spike starts from 0 (respectively 1), while the condition $\bar{q}_{t-} \neq \bar{q}_t$ corresponds to a jump for the process $\bar{q}_t$.

Observe also that in this general context (not motivated by quantum physics), to adapt the analytical proofs developed in this paper, we would need the following:

(1) to have a resetting dynamics, i.e., $G(q) = q^* - q$, $q^* \in (0, 1)$;

(2) to have a good understanding of the deterministic flow $\hat{q}^\gamma$ defined by $\dot{\hat{q}}_t^\gamma = F(\hat{q}_t^\gamma) - \gamma G(\hat{q}_t^\gamma)H(\hat{q}_t^\gamma)$ for large γ.

Note that the collapse-unitary case considered in Secs. IV and V A is not in the form of our general setup (62) on [0,1]. To transform Eq. (18) to an equation on the line as in Eq. (62), we need to come back to the usual coordinate q^γ in Eq. (14). With the notations of Sec. IV, the plane $\varphi_t = \frac{\pi}{2}$ is stable, and then by restricting the dynamics to this plane, we find the equation

$$\dot{q}_t^\gamma = F_\gamma\big(q_t^\gamma\big) + G\big(q_t^\gamma\big)\big(\dot{\mathcal{N}}_t^\gamma - \gamma H\big(q_t^\gamma\big)\big), \tag{66}$$

with

$$F_\gamma(q) = 2k_\gamma\sqrt{q(1-q)}, \quad G(q) = -q, \quad H(q) = \eta(1-q),$$

and $\mathcal{N}^\gamma$ is a Poisson process satisfying

$$\mathbb{E}\big(d\mathcal{N}_t^\gamma|q_t^\gamma\big) = \gamma H\big(q_t^\gamma\big)dt, \quad d\mathcal{N}_t^\gamma d\mathcal{N}_t^\gamma = d\mathcal{N}_t^\gamma. \tag{67}$$

At first sight, Eq. (66) is directly in the form (62) if k_γ is γ independent, but then the general previous conjecture gives that there are no jumps and no spikes because $F(0) = 0 = F(1)$ in Eq. (67) (Zeno effect). On the other hand, if $k_\gamma = \sqrt{\omega\gamma}$ as we did in Secs. IV and V A, then $F_\gamma(q) = 2\sqrt{\gamma}\sqrt{\omega q(1-q)}$ and the factor $\sqrt{\gamma}$ breaks the validity of the conjecture.

Following we first give, in Sec. VI A, some nonquantum motivated examples where we numerically verify the above conjecture. In Sec. VI B we discuss a nontrivial quantum example where we expect the conjecture to be true but our analytical approach based on resetting cannot be applied. Finally, in Sec. VI C we discuss a generalization of Eq. (62) in the context of collapse-measurement setup.

A. Example 1 with resetting: Nonquantum SDEs

In the general Markovian 1D piecewise deterministic process given by Eq. (62), we numerically study the emergence of spikes for large γ. In the context of resetting dynamics to a point q^*, we require $G(q) = q^* - q$. If $q^* \neq 0$ and $q^* \neq 1$, the hypothesis (63) will only be satisfied if $H(0) = H(1) = 0$, in which case the intensity of the spiking process vanishes. Thus, to observe spikes, we take $q^* = 0$ without loss of generality. In addition, to satisfy Eq. (63), we need then to take $H(1) = 0$, so we consider $H(q) = (1-q)\chi(q)$, where $\chi(q)$ is any finite function such that $\chi(0) \neq 0$. Then the conjecture (65) gives that $P_c[n : (s,t), a, b]$ converge at large γ to a Poisson distribution limit (65) with intensity parameter given by (one-sided spikes)

$$\lambda^{\bar{q}}_{[a,b]} = \begin{cases} \int_a^b dx \frac{|F(0)|}{x^2}, & \text{if} \quad \bar{q}\,|_{[s,t]} = 0 \\ 0, & \text{if} \quad \bar{q}\,|_{[s,t]} = 1. \end{cases}$$

In Fig. 10, we numerically verify the conjecture by taking $\chi(q)$ to be a fourth-order polynomial with arbitrary coefficients, for two very different forms of $F(q)$: (i) $F(q) = \cos(\frac{50q}{\pi})$, a highly oscillatory function and (ii) $F(q) = (e^{-q} - 0.5)$, a strictly monotonic function.

B. Example 2 without resetting: Collapse-thermal setup with general QND (diagonal) measurement N_1 operator

Consider the collapse-thermal setup for a qubit with a general diagonal measurement operator (intensity is denoted by γ and efficiency by η)

$$N_1 = \begin{pmatrix} n_+ & 0 \\ 0 & n_- \end{pmatrix}.$$

By using the computations performed in Appendix A, we easily get that, with the usual parametrization of the density matrix ρ_t^γ given in Eq. (10),

$$\begin{aligned} \dot{q}_t^\gamma &= (W_{+,-} + W_{-,+})\left(\frac{W_{-,+}}{W_{+,-} + W_{-,+}} - q_t^\gamma\right) \\ &\quad + \frac{|n_+|^2 - |n_-|^2}{(|n_+|^2 - |n_-|^2)q_t^\gamma + |n_-|^2} \\ &\quad \times \big(1 - q_t^\gamma\big)q_t^\gamma\left[\dot{\mathcal{N}}_t^\gamma - \mathbb{E}\big(\dot{\mathcal{N}}_t^\gamma|q_t^\gamma\big)\right], \end{aligned} \tag{68}$$

with $d\mathcal{N}_t^\gamma d\mathcal{N}_t^\gamma = d\mathcal{N}_t^\gamma$,

$$\mathbb{E}\big(d\mathcal{N}_t^\gamma|q_t^\gamma\big) = \gamma\eta[(|n_+|^2 - |n_-|^2)\,q_t^\gamma + |n_-|^2]dt. \tag{69}$$

Observe that Eq. (68) takes the form of Eq. (62) with

$$\begin{aligned} F(q) &= (W_{+,-} + W_{-,+})\left(\frac{W_{-,+}}{W_{+,-} + W_{-,+}} - q_t^\gamma\right), \\ G(q) &= \frac{|n_+|^2 - |n_-|^2}{(|n_+|^2 - |n_-|^2)q + |n_-|^2}\,(1-q)q, \\ H(q) &= \eta[(|n_+|^2 - |n_-|^2)\,q + |n_-|^2]. \end{aligned} \tag{70}$$

In particular, for the model considered in Eq. (20), i.e., $n_+ = 0$, $n_- = 1$ (resetting dynamics), we have that our conjecture is satisfied with spikes only from 0 and spikes statistics described by the spike process $\mathbb{Q}$ defined in Eq. (64). But our

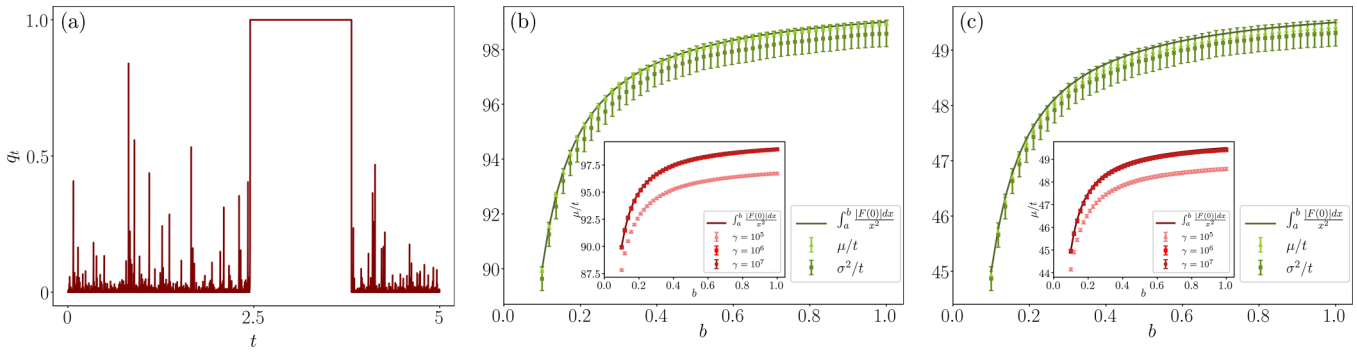

FIG. 10. (a) The typical trajectory for the general 1D PDMP Eq. (62) with resetting to $q^* = 0$ for $\gamma = 10^4$. The jumps between $q_t = 0$ and 1 are interspersed with spikes from $q_t = 0$ in the strong measurement limit. In (b) and (c), we plot the mean and variance of the distribution (conditioned on no jumps) of the number of spikes (from $q_t = 0$) per unit time in a space-time box $(0.01, b) \times (0, t)$ against the box edge b for (b) $F(q) = \cos(\frac{50q}{\pi})$ and (c) $F(q) = (e^{-q} - 0.5)$. This empirically verifies the conjecture that the spiking process is Poissonian with the parameter $\int_a^b \frac{|F(0)|dx}{x^2}$. The data points were obtained for the parameters $t = 0.1$ and $\gamma = 10^7$ by averaging over 10^5 realizations with $dt = 6.25 \times 10^{-11}$. The data in the insets show the convergence of the empirical mean and time to the conjectured value as γ is increased.

conjecture claims that, moreover, in general (even without resetting dynamics), there are spikes starting from 0 and from 1. This is the case if $F(0)H(0) = \eta W_{-,+}|n_-|^2 \neq 0$ (spikes from 0 to 1) and $F(1)H(1) = \eta W_{+,-}|n_+|^2 \neq 0$ (spikes from 1 to 0). This is confirmed by numerical simulations (see Fig. 11).

Observe moreover that if we consider the measurement operator $N_1 = \sigma_z$ (hence $|n_-|^2 = |n_+|^2$), as it was considered in the Gaussian case [52–54,56], we get a purely deterministic equation without jumps or spikes. This is very different from the studies cited previously in the Gaussian noise context.

C. Example 3 with resetting: Collapse-measurement setup for QND resetting $N_1 = |-\rangle\langle -|$ but general N_2 operator

To generalize the collapse-measurement setup given by Eq. (23), we can substitute the damping-spontaneous emission operator N_2, defined in Eq. (21), by a general (not necessarily diagonal) measurement operator N_2 (in order to break the QND assumption). Then, we can check that, generically, the equation for q^γ is not autonomous. More exactly, the non-commutativity of N_2 with respect to N_1 (to break the QND assumption) and the fact that q^γ has an autonomous evolution, are equivalent to taking N_2 in the form

$$N_2 = \begin{pmatrix} 0 & a \\ b & 0 \end{pmatrix}, \quad ab \neq 0. \tag{71}$$

The requirement that q^γ has an autonomous evolution seems to be a necessary condition to adapt our analytical proof (technical assumption).

Observe, however that, even in this case, the collapse-measurement setup does not fall directly in our conjecture case (62) because we have then two Poisson noises involved (but the second one is weaker than the first one since γ_2 is of order one while γ_1 is very large). More precisely, the equation for q^γ is given by (Appendix B)

$$\dot{q}_t^\gamma = F(q_t^\gamma) + G_1(q_t^\gamma)\big(\dot{\mathcal{N}}_t^{1,\gamma} - \gamma_1 H_1(q_t^\gamma)\big) + G_2(q_t^\gamma)\dot{\mathcal{N}}_t^{2,\gamma}, \tag{72}$$

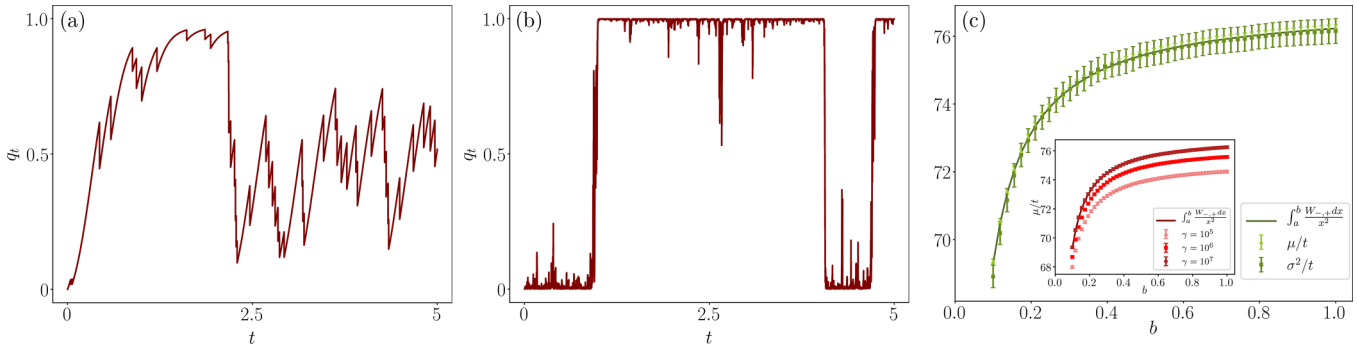

FIG. 11. The typical trajectory for (a) $\gamma = 10^2$ and (b) $\gamma = 10^4$ for the collapse-thermal setup for a general measurement operator for the parameters $|n_+|^2 = 0.2$, $|n_-|^2 = 0.4$, $W_{-,+} = 0.77$, $W_{+,-} = 0.23$. Here, (b) shows that the jumps between $q_t = 0$ and 1 are interspersed with spikes from both $q_t = 0$ and 1 in the strong measurement limit, even though the dynamics in this case does not reset to a fixed point. In (c), we plot the mean and variance of the distribution (conditioned on no jumps) of the number of spikes (from $q_t = 0$) per unit time in a space-time box $(0.01, b) \times (0, t)$ against the box edge b for the same set of parameters. This empirically verifies the conjecture that the spiking process is Poissonian with the parameter $\int_a^b \frac{W_{-,+}dx}{x^2}$. The data points were obtained for the parameters $t = 0.1$ and $\gamma = 10^7$ by averaging over 10^5 realizations with $dt = 10^{-9}$. The data in the inset show the convergence of the empirical mean and time to the conjectured value as γ is increased.

with

$$F(q) = \gamma_2\{|a|^2 - (|a|^2 + |b|^2)q\}\{1 - \eta_2 G_2(q)\},$$
$$G_2(q) = \frac{|a|^2(1-q)}{|a|^2(1-q) + |b|^2 q} - q,$$
$$H_2(q) = \eta_2[|a|^2(1-q) + |b|^2 q],$$
$$G_1(q) = -q,$$
$$H_1(q) = \eta_1(1-q),$$

and the Poisson noises satisfy

$$\mathbb{E}\big(d\mathcal{N}_t^{k,\gamma} \big| q_t^\gamma\big) = H_k\big(q_t^\gamma\big)dt,$$
$$d\mathcal{N}_t^{k,\gamma} d\mathcal{N}_t^{\ell,\gamma} = \delta_{k\ell}\, d\mathcal{N}_t^{k,\gamma}.$$

Hence, a stronger conjecture of the one above is that, if we have an evolution equation given by Eq. (72) with hypothesis (63), then in the large limit $\gamma_1 \to \infty$, γ_2 of order 1, the graph of q^γ should converge to a spiking process $\mathbb{Q}$, given by Eq. (64) with H replaced there by the dominant term H_1. Since $F(1)H_1(1) = 0$, we expect only to have no spikes from 1 [apart from the degenerate case $\gamma_2|a|^2(1-\eta_2) = 0$, see below, we will always have spikes from 0].

In this paper, we considered only N_2 equal to the damping-spontaneous emission operator appearing in Eq. (21), which corresponds to the case $a = 1$ and $b = 0$, and then the previous conjecture about the spike statistics is in agreement with the third relation in Eq. (25) because $F(0) = \gamma_2(1-\eta_2)$. Another standard rank-one choice is to take N_2 equal to the spontaneous absorption operator given by

$$N_2 = \begin{pmatrix} 0 & 0 \\ 1 & 0 \end{pmatrix} = |-\rangle\langle +|.$$

In the latter case ($a = 0, b = 1$) we have then a competition between a strong resetting dynamics and a weak resetting dynamics towards the same $|-\rangle\langle -|$. Our conjecture implies thus that in this case, we do not have spikes but only jumps.

VII. CONCLUSION

In this work, we discussed finite-dimensional quantum trajectories driven by Poissonian noises [see Eq. (1)] in a strong measurement limit and focused our studies to a qubit system in three different setups where the quantum-nondemolition condition for the strong measurement is broken by a unitary evolution, a thermal bath, or a second measurement (see Sec. III). Our analytical studies of Sec. V establish that the quantum trajectory investigated behaves like a pure jump Markov process in the strong measurement limit. However, this rough picture can be refined and it appears in fact that this quantum jump Markov process is in fact decorated by vertical lines (called spikes). The first analytical description of spikes was done recently by Bauer-Bernard-Tilloy [52–54], and motivated some others works [55,56], but in the context of quantum trajectories of a qubit driven by a Gaussian noise.

Observe that in all the setups we studied analytically, we observe a kind of universal law for the distribution of spikes [see Eq. (24)], valid for Gaussian or Poissonian noises. Numerical experiments confirm our analytical results.

A fundamental property used to perform our analytical investigation in Sec. V is that the evolution of the quantum trajectory can be reduced to the evolution of a one-dimensional piecewise Markovian deterministic process with resetting. Hence, apart from its interest in this quantum framework, this problem could be subject of investigation in the resetting literature. Moreover, it seems that the existence of spikes is more generic and they can appear in other piecewise Markovian deterministic processes which do not have a resetting property (see, e.g., Fig. 11). In Sec. VI we provide a general conjecture for the distribution of the spikes in a general one-dimensional framework.

Quantum trajectories are now routinely realized in experiments [25–30,78], but the question of whether spikes can be experimentally detected remains open. A few remarks on how this work addresses this question are in order. First, spikes emerge in the $\gamma \to \infty$ limit, but their statistical properties can be observed for large but finite γ, as evidenced by our numerical results. These are obtained by the counting statistics of "prespikes." Second, for the quantum trajectories of the kind considered in this work, the dynamics consists of a deterministic flow with intermittent resetting to a particular state. This dynamics does not merely arise from a toy model, but has its basis in modern day experiments [79]. Finally, one can truly claim the experimental detection of spikes only if one can infer the statistics of the spikes (or, more precisely, the prespikes) *without relying on the stochastic master equation*. This would take the observation of spikes out of the realm of simulations and into a laboratory. To achieve this, one can consider the quantum trajectory that was experimentally realized in [79]. Although that particular quantum trajectory had Gaussian noise, the experiment demonstrated highly efficient detection of clicks (transitions to the ground state) and, moreover, by performing quantum state tomography over an ensemble of no-click trajectories, the state was shown to follow a fixed path through the Hilbert space during the no-click evolution. Using the knowledge of this path and the click sequence records, it is in principle possible to infer the statistics of the heights of the prespikes. However, there are a few subtleties associated with this proposal, one of them being that the system in [79] was essentially a qutrit. We expect that spikes can occur in higher-dimensional quantum systems, but it is not known whether they have the same power-law statistics as the qubit case. These are questions that we hope to address in a future work.

ACKNOWLEDGMENTS

We thank M. Bauer, R. Chhaibi, and C. Pellegrini for useful discussions. This work was supported by the projects RETENU ANR-20-CE40 of the French National Research Agency (ANR). A.S. and A.D. acknowledge financial support of the Department of Atomic Energy, Government of India, under Project Identification No. RTI 4001. A.K. acknowledges financial support for Project No. NDFluc U-AGR-7239-00-C from the Luxembourg National Research Fund, Fonds National de la Recherche. A.D. acknowledges the J.C. Bose Fellowship (Grant No. JCB/2022/000014) of the Science and Engineering Research Board of the Department of Science and Technology, Government of India. A.D. and A.K. thank

Laboratoire J A Dieudonné and INPHYNI, Nice, for supporting a visit which initiated this project. A.D. thanks the National Research University Higher School of Economics, Moscow, for supporting a visit. R.C. thanks ICTS-TIFR for supporting a visit for the completion of the project.

APPENDIX A: MEASUREMENT PART OF THE SME EQ. (1) FOR QUBIT WITH A GENERAL DIAGONAL MEASUREMENT OPERATOR

We perform here computations in a more general framework where the measurement operator N is still diagonal

$$N = \begin{pmatrix} n_+ & 0 \\ 0 & n_- \end{pmatrix}$$

but not necessarily of rank one like in Eq. (7). We consider hence only the dynamics generated by the measurement operator N with intensity $\gamma > 0$ and efficiency η:

$$\dot{\rho}_t^\gamma = \gamma L_N[\rho_t^\gamma] + M_N[\rho_t^\gamma]\big[\dot{\mathcal{N}}_t^\gamma - \gamma\eta\,\mathrm{Tr}\big(N\rho_t^\gamma N^\dagger\big)\big] \tag{A1}$$

with the noise $\mathcal{N}_t^\gamma$ satisfying $d\mathcal{N}_t^\gamma \in \{0,1\}$, $d\mathcal{N}_t^\gamma d\mathcal{N}_t^\gamma = d\mathcal{N}_t^\gamma$, and

$$\mathbb{E}\big(d\mathcal{N}_t^\gamma \big| \rho_t^\gamma\big) = \eta\gamma\,\mathrm{Tr}\big(N\rho_t^\gamma N^\dagger\big)dt\ . \tag{A2}$$

We use the usual parametrization of the density matrix ρ_t^γ given in Eq. (10). Then Eq. (A1) takes the form of a three-dimensional (because even if q^γ is real, u^γ is complex) PDMP

$$\begin{aligned} \dot{q}_t^\gamma &= \alpha\big(q_t^\gamma\big)\,\big[\dot{\mathcal{N}}_t^\gamma - \mathbb{E}\big(\dot{\mathcal{N}}_t^\gamma \big| q_t^\gamma\big)\big], \\ \dot{u}_t^\gamma &= -\frac{\gamma}{2}(|n_+|^2 + |n_-|^2 - 2\overline{n_+}n_-)u_t^\gamma \\ &\quad + \beta\big(q_t^\gamma\big)\,u_t^\gamma\big[\dot{\mathcal{N}}_t^\gamma - \mathbb{E}\big(\dot{\mathcal{N}}_t^\gamma \big| q_t^\gamma\big)\big] \end{aligned} \tag{A3}$$

with

$$\begin{aligned} \alpha\big(q_t^\gamma\big) &= \frac{(|n_+|^2 - |n_-|^2)q_t^\gamma\big(1-q_t^\gamma\big)}{(|n_+|^2 - |n_-|^2)q_t^\gamma + |n_-|^2}, \\ \beta\big(q_t^\gamma\big) &= \frac{\overline{n_+}n_-}{(|n_+|^2 - |n_-|^2)q_t^\gamma + |n_-|^2} - 1, \end{aligned} \tag{A4}$$

and

$$\begin{aligned} \mathbb{E}\big(d\mathcal{N}_t^\gamma \big| q_t^\gamma\big) &= \gamma\eta\{(|n_+|^2 - |n_-|^2)q_t^\gamma + |n_-|^2\}\,dt, \\ d\mathcal{N}_t^\gamma d\mathcal{N}_t^\gamma &= d\mathcal{N}_t^\gamma. \end{aligned}$$

Observe that the diagonal dynamics is autonomous.

1. Resetting dynamics or not

The transition rate of the Poisson noise in Eq. (A1) is given by

$$\begin{aligned} W((q,p)\to,(q',p')) = \gamma\eta[(|n_+|^2 - |n_-|^2)q + |n_-|^2] \\ \times\delta\left(q' - \frac{|n_+|^2 q}{(|n_+|^2 - |n_-|^2)q + |n_-|^2}\right) \\ \times\delta\left(p' - \frac{\overline{n_+}n_- p}{(|n_+|^2 - |n_-|^2)q + |n_-|^2}\right). \end{aligned} \tag{A5}$$

Observe that these jumps correspond to a resetting dynamics towards a point if and only if for any q, p we have that

$$\begin{aligned} \frac{|n_+|^2 q}{(|n_+|^2 - |n_-|^2)q + |n_-|^2} &= k_1, \\ \frac{\overline{n_+}n_- p}{(|n_+|^2 - |n_-|^2)q + |n_-|^2} &= k_2, \end{aligned}$$

where k_1, k_2 are two arbitrary fixed constants, i.e., independent of q, p. We show easily that there are only two possibilities to have that. The first one is that

$$k_1 = 0 = k_2, \quad n_+ = 0, \quad \text{i.e.,} \quad N = \begin{pmatrix} 0 & 0 \\ 0 & 1 \end{pmatrix} = N_1,$$

and the second one is

$$k_1 = 1, \quad k_2 = 0, \quad n_- = 0, \quad \text{i.e.,} \quad N = \begin{pmatrix} 1 & 0 \\ 0 & 0 \end{pmatrix}.$$

2. Proof of Eq. (A3)

The proof is based on elementary algebraic computations. We have that the Lindbladian term is given by

$$\begin{aligned} L_N[\rho_t^\gamma] &= N\rho_t^\gamma N^\dagger - \frac{1}{2}N^\dagger N\rho_t^\gamma - \frac{1}{2}\rho_t^\gamma N^\dagger N \\ &= \begin{pmatrix} 0 & -\frac{|n_+|^2+|n_-|^2-2n_+\overline{n_-}}{2}\overline{u}_t^\gamma \\ -\frac{|n_+|^2+|n_-|^2-2\overline{n_+}n_-}{2}u_t^\gamma & 0 \end{pmatrix}. \end{aligned}$$

The "stochastic innovation" term is given by

$$M_N[\rho_t^\gamma] = \frac{N\rho_t^\gamma N^\dagger}{\mathrm{Tr}\big(N\rho_t^\gamma N^\dagger\big)} - \rho_t^\gamma = \begin{pmatrix} \alpha\big(q_t^\gamma\big) & \bar{\beta}\big(q_t^\gamma\big)\,\overline{u}_t^\gamma \\ \beta\big(q_t^\gamma\big)\,u_t^\gamma & -\alpha\big(q_t^\gamma\big) \end{pmatrix},$$

where α, β have been defined in Eq. (A4).

APPENDIX B: PROOF OF EQS. (72) AND (23)

We consider Eq. (71):

$$N_2 = \begin{pmatrix} 0 & a \\ b & 0 \end{pmatrix}, \quad ab \neq 0. \tag{B1}$$

Observe that

$$\begin{aligned} L_{N_2}[\rho_t^\gamma] &= N_2\rho_t^\gamma N_2^\dagger - \frac{1}{2}N_2^\dagger N_2\rho_t^\gamma - \frac{1}{2}\rho_t^\gamma N_2^\dagger N_2 \\ &= \begin{pmatrix} |a|^2\big(1-q_t^\gamma\big) - |b|^2 q_t^\gamma & a\bar{b}u_t^\gamma - \frac{|b|^2+|a|^2}{2}\overline{u_t^\gamma} \\ \bar{a}b\overline{u_t^\gamma} - \frac{|b|^2+|a|^2}{2}u_t^\gamma & |b|^2 q_t^\gamma - |a|^2\big(1-q_t^\gamma\big) \end{pmatrix} \end{aligned}$$

and

$$\begin{aligned} M_{N_2}[\rho_t^\gamma] &= \frac{N_2\rho_t^\gamma N_2^\dagger}{\mathrm{Tr}\big(N_2\rho_t^\gamma N_2^\dagger\big)} - \rho_t^\gamma \\ &= \begin{pmatrix} \frac{|a|^2(1-q_t^\gamma)}{|a|^2(1-q_t^\gamma)+|b|^2 q_t^\gamma} - q_t^\gamma & \frac{a\bar{b}u_t^\gamma}{|a|^2(1-q_t^\gamma)+|b|^2 q_t^\gamma} - \overline{u_t^\gamma} \\ \frac{\bar{a}b\overline{u_t^\gamma}}{|a|^2(1-q_t^\gamma)+|b|^2 q_t^\gamma} - u_t^\gamma & \frac{|b|^2 q_t^\gamma}{|a|^2(1-q_t^\gamma)+|b|^2 q_t^\gamma} - 1 + q_t^\gamma \end{pmatrix}. \end{aligned}$$

Then, with the Eq. (11) for the N_1-measurement part, we obtain finally Eq. (72). In the particular case of spontaneous emission (21),

$$N_2 = \begin{pmatrix} 0 & 1 \\ 0 & 0 \end{pmatrix} = |+\rangle\langle -|, \tag{B2}$$

Eq. (11) becomes Eq. (23).

APPENDIX C: PROOF OF EQ. (17)

We consider the SME (1) in the collapse-unitary setup (12) [see Eq. (14) with the usual parametrization of the density matrix ρ_t^γ given in Eq. (10)]. To simplify notation, we denote now γ_1 by γ by η, $\mathcal{N}_t^{\gamma,1}$ by $\mathcal{N}_t^\gamma$.

Parametrizing now the density matrix in Bloch coordinates [Eq. (15)], we prove below that

$$\frac{d}{dt}\big(r_t^\gamma\big)^2 = \gamma(\eta-1)2\big(1-q_t^\gamma\big)\big[\big(r_t^\gamma\big)^2+2q_t^\gamma-1\big] + \big[1-\big(r_t^\gamma\big)^2\big]\big[\gamma\big(2q_t^\gamma-1\big)+\dot{\mathcal{N}}_t^\gamma\big]. \tag{C1}$$

Then, we can conclude that if the measurement is totally efficient, i.e., $\eta=1$, then the Bloch sphere $r=1$ (pure states) is stable under the dynamics. We will restrict us to this case now, i.e., pure state dynamics ($r_t^\gamma=1$) and totally efficient $\eta=1$.

The Bloch sphere of pure states can be parametrized with the angles $\theta_t^\gamma\in(-\pi,\pi]$, $\varphi_t^\gamma\in[0,\pi]$ [see Eq. (15)]:

$$q_t^\gamma=\cos^2\left(\tfrac{\theta_t^\gamma}{2}\right),\quad u_t^\gamma=\frac{\big(\sin\theta_t^\gamma\big)}{2}e^{i\varphi_t^\gamma}. \tag{C2}$$

We then look for an SDE for $(\theta_t^\gamma,\varphi_t^\gamma)$ which gives a solution to the SDE (14). We claim that if $(\theta_t^\gamma,\varphi_t^\gamma)$ satisfies the SDE

$$\begin{aligned}\dot\theta_t^\gamma&=\big[-2k_\gamma\sin\big(\varphi_t^\gamma\big)-\frac{\gamma}{2}\sin\big(\theta_t^\gamma\big)\big]+\big(\pi-\theta_t^\gamma\big)\dot{\mathcal{N}}_t^\gamma,\\ \dot\varphi_t^\gamma&=-2k_\gamma\frac{\cos\big(\theta_t^\gamma\big)}{\sin\big(\theta_t^\gamma\big)}\cos\big(\varphi_t^\gamma\big)\end{aligned} \tag{C3}$$

with

$$\mathbb{E}\big(d\mathcal{N}_t^\gamma\big|\theta_t^\gamma\big)=\gamma\left(\sin\frac{\theta_t^\gamma}{2}\right)^2dt,\quad d\mathcal{N}_t^\gamma d\mathcal{N}_t^\gamma=d\mathcal{N}_t^\gamma,$$

then (q_t^γ,u_t^γ) defined through Eq. (C2) satisfied the SDE (14).

To prove this claim, it is sufficient to apply the Ito-jump stochastic calculus [80,81]. In fact, we see that the SDE (C3) is not well defined when $\theta_t^\gamma=\pi$, so that some extra boundary conditions should be added to define it correctly. This is due to the fact that the change of variable (C2) is not smooth. However, in the particular case we consider, where $\varphi_t^\gamma=\pi/2$, we can disregard this technical issue.

1. Proof of Eq. (C1)

We have $(r_t^\gamma)^2=(2q_t^\gamma-1)^2+4u_t^\gamma\bar u_t^\gamma$ and then with Ito-jump stochastic calculus

$$\begin{aligned}d(r_t^\gamma)^2&=d\big[\big(2q_t^\gamma-1\big)^2+4u_t^\gamma\bar u_t^\gamma\big]\\&=4\big(2q_t^\gamma-1\big)\big(dq_t^\gamma\big)_c+4\big(du_t^\gamma\big)_c\bar u_t^\gamma+4u_t^\gamma\big(d\bar u_t^\gamma\big)_c\\&\quad+\big[2\big(q_t^\gamma-q_t^\gamma d\mathcal{N}_t^\gamma\big)-1\big]^2-\big(2q_t^\gamma-1\big)^2\\&\quad+4\big[\big(u_t^\gamma-q_t^\gamma d\mathcal{N}_t^\gamma\big)\big(\bar u_t^\gamma-q_t^\gamma d\mathcal{N}_t^\gamma\big)-u_t^\gamma\bar u_t^\gamma\big]\end{aligned}$$

with

$$\begin{aligned}\big(dq_t^\gamma\big)_c&=ik_\gamma\big(u_t^\gamma-\bar u_t^\gamma\big)+\gamma\eta q_t^\gamma\big(1-q_t^\gamma\big),\\\big(du_t^\gamma\big)_c&=-ik_\gamma\big(2q_t^\gamma-1\big)-\frac{\gamma}{2}u_t^\gamma+\gamma\eta u_t^\gamma\big(1-q_t^\gamma\big),\\\big(d\bar u_t^\gamma\big)_c&=+ik_\gamma\big(2q_t^\gamma-1\big)-\frac{\gamma}{2}\bar u_t^\gamma+\gamma\eta\bar u_t^\gamma\big(1-q_t^\gamma\big).\end{aligned}$$

We have

$$\begin{aligned}d\big(r_t^\gamma\big)^2&=d\big(\big(2q_t^\gamma-1\big)^2+4u_t^\gamma\bar u_t^\gamma\big)\\&=4\big(2q_t^\gamma-1\big)dq_t^\gamma+4\big(dq_t^\gamma\big)\big(dq_t^\gamma\big)+4\big(du_t^\gamma\big)\bar u_t^\gamma\\&\quad+4u_t^\gamma\big(d\bar u_t^\gamma\big)+4\big(du_t^\gamma\big)\big(d\bar u_t^\gamma\big)\\&=4\big(2q_t^\gamma-1\big)\big\{\big[-ik_\gamma\big(u_t^\gamma-\bar u_t^\gamma\big)+\gamma\eta\big(1-q_t^\gamma\big)q_t^\gamma\big]dt\\&\quad-q_t^\gamma d\mathcal{N}_t^\gamma\big\}\\&\quad+4\big(q_t^\gamma\big)^2d\mathcal{N}_t^\gamma\\&\quad+4\big\{\big[-ik_\gamma\big(2q_t^\gamma-1\big)\bar u_t^\gamma+\gamma\big(-\tfrac12+\eta-\eta q_t^\gamma\big)u_t^\gamma\bar u_t^\gamma\big]dt\\&\quad-u_t^\gamma\bar u_t^\gamma d\mathcal{N}_t^\gamma\big\}\\&=\gamma(\eta-1)2\big(1-q_t^\gamma\big)\big[\big(r_t^\gamma\big)^2+2q_t^\gamma-1\big]\\&\quad+\big[1-\big(r_t^\gamma\big)^2\big]\big[\gamma\big(2q_t^\gamma-1\big)dt+d\mathcal{N}_t^\gamma\big].\end{aligned}$$

APPENDIX D: CONVERGENCE OF SPIKING PROCESS FOR THE SCALING $k_\gamma\sim\gamma^\alpha$

We discuss the motivation behind the choice of $k_\gamma=\sqrt{\omega\gamma}$ in the collapse-unitary case in the main text. From numerical simulations (see Fig. 12), we determine that for the scaling $k_\gamma\sim\gamma^\alpha$, the distribution of the spiking process does not converge for large γ for $\alpha\gtrapprox0.5$ and the spikes vanish for large γ for $\alpha\lessapprox0.5$. This can also be seen by taking the limits $\omega\to0$ and $\omega\to\infty$ in the first line of Eq. (25) (corresponding to $\alpha<0.5$ and $\alpha>0.5$, respectively). This provides credible justification for the form of k_γ that was assumed in the main text.

APPENDIX E: EXACT COMPUTATION AND ASYMPTOTICS OF LAPLACE TRANSFORMS

1. Collapse-unitary setup

We derive the explicit expressions for the functions $C(\sigma)$, $D(\sigma)$, and $E(\sigma)$ (and their asymptotic forms for large γ) to determine the generating function of the distribution of spikes for the collapse-unitary case. Thanks to the explicit expressions (35), we have then that

$$\begin{aligned}E(\sigma)=\frac{1}{4(\beta')^2}\Bigg\{&\frac{1+e^{-2\phi}}{\sigma+\gamma/2-2\beta k_\gamma}\big(1-e^{-(\sigma+\gamma/2-2\beta k_\gamma)\tau}\big)\\&+\frac{1+e^{2\phi}}{\sigma+\gamma/2+2\beta k_\gamma}\big(1-e^{-(\sigma+\gamma/2+2\beta k_\gamma)\tau}\big)\\&-\frac{4}{\sigma+\gamma/2}\big(1-e^{-(\sigma+\gamma/2)\tau}\big)\Bigg\},\end{aligned} \tag{E1}$$

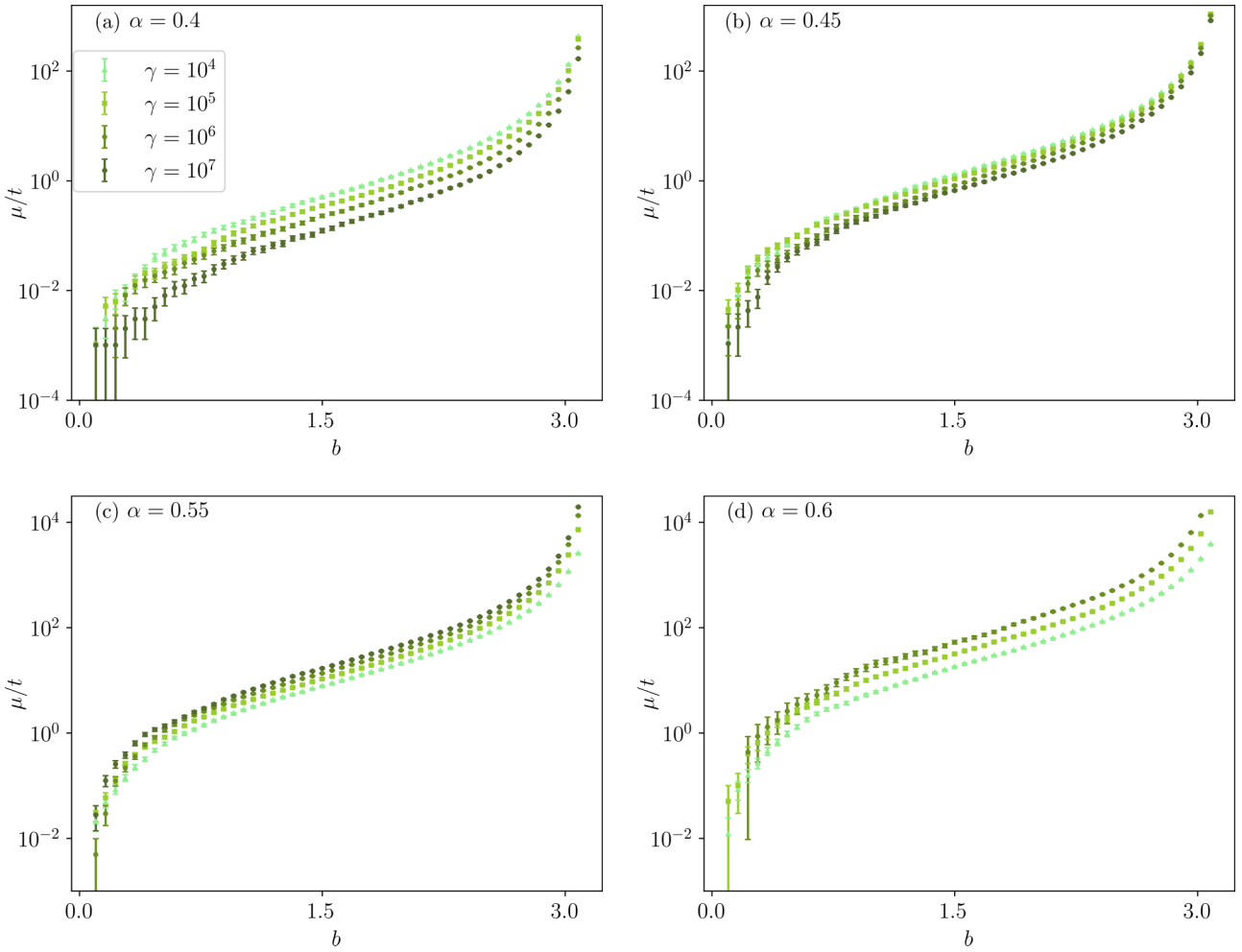

FIG. 12. Mean of the distribution (conditioned on no jumps) of the number of spikes (from $\theta_t = \pi$) per unit time in a space-time box $(0, b) \times (0, t)$ plotted against the box edge b for (a) $k_\gamma \sim \gamma^{0.4}$, (b) $k_\gamma \sim \gamma^{0.45}$, (c) $k_\gamma \sim \gamma^{0.55}$, and (d) $k_\gamma \sim \gamma^{0.6}$. The separation between the scatter plots for various γ is more than the width of the error bars and clearly indicates a downward trend with increasing γ for $\alpha = 0.4$ and 0.45 (indicating that the spikes vanish for $\gamma \to \infty$) and clearly indicates an upward trend with increasing γ for $\alpha = 0.55$ and 0.6 (indicating that the moments of the spike distribution diverge for $\gamma \to \infty$). The data points were obtained by averaging over 10^4 realizations. Note that for $\alpha = 0.6$, we were not able to obtain data for $\gamma = 10^7$ since almost all the trajectories in the sample had the occurrence of jumps (recall that the spike distribution is conditioned on no jumps).

$$C(\sigma) + D(\sigma) = \frac{\gamma}{4(\beta')^2}\left\{\frac{e^{-2\phi}}{\sigma + \gamma/2 - 2\beta k_\gamma}(1 - e^{-(\sigma+\gamma/2-2\beta k_\gamma)\tau}) + \frac{e^{2\phi}}{\sigma + \gamma/2 + 2\beta k_\gamma}(1 - e^{-(\sigma+\gamma/2+2\beta k_\gamma)\tau}) - \frac{2}{\sigma + \gamma/2}(1 - e^{-(\sigma+\gamma/2)\tau})\right\} \tag{E2}$$

and

$$D(\sigma) = \left\{\frac{e^{-2\phi}}{\sigma + \gamma/2 - 2\beta k_\gamma}(e^{-(\sigma+\gamma/2-2\beta k_\gamma)\tau_b} - e^{-(\sigma+\gamma/2-2\beta k_\gamma)\tau_a}) + \frac{e^{2\phi}}{\sigma + \gamma/2 + 2\beta k_\gamma}(e^{-(\sigma+\gamma/2+2\beta k_\gamma)\tau_b} - e^{-(\sigma+\gamma/2+2\beta k_\gamma)\tau_a}) - \frac{2}{\sigma + \gamma/2}(e^{-(\sigma+\gamma/2)\tau_b} - e^{-(\sigma+\gamma/2)\tau_a})\right\} \times \frac{\gamma}{4(\beta')^2}. \tag{E3}$$

We note the asymptotic forms for large γ (here we take $k_\gamma = \sqrt{\omega\gamma}$):

$$C(\sigma) \sim 1 - (4\omega + \sigma)\gamma^{-1} - D(\sigma), \quad D(\sigma) \sim 4\omega\gamma^{-1}[\tan^2(b/2) - \tan^2(a/2)], \quad E(\sigma) \sim \gamma^{-1}. \tag{E4}$$

Then Eq. (42) follows.

2. Collapse-thermal setup

We derive the explicit expressions for the functions $C(\sigma)$, $D(\sigma)$, and $E(\sigma)$ (and their asymptotic forms for large γ) to determine the generating function of the distribution of spikes for the collapse-thermal case. Thanks to Eq. (50) we have that

$$E(\sigma) = \frac{1}{q_+ - q_-}\left\{\frac{q_+(1-e^{-[\sigma+\eta\gamma(1-q_-)]\tau})}{\sigma+\eta\gamma(1-q_-)} - \frac{q_-(1-e^{-[\sigma+\eta\gamma(1-q_+)]\tau})}{\sigma+\eta\gamma(1-q_+)}\right\}, \tag{E5}$$

$$C(\sigma)+D(\sigma) = \frac{\gamma\eta}{q_+ - q_-}\left\{\frac{q_+(1-q_-)(1-e^{-[\sigma+\eta\gamma(1-q_-)]\tau})}{\sigma+\eta\gamma(1-q_-)} - \frac{q_-(1-q_+)(1-e^{-[\sigma+\eta\gamma(1-q_+)]\tau})}{\sigma+\eta\gamma(1-q_+)}\right\}, \tag{E6}$$

and

$$D(\sigma) = \frac{\gamma\eta}{q_+ - q_-}\left\{\frac{q_+(1-q_-)(e^{-[\sigma+\eta\gamma(1-q_-)]\tau_a}-e^{-[\sigma+\eta\gamma(1-q_-)]\tau_b})}{\sigma+\eta\gamma(1-q_-)} - \frac{q_-(1-q_+)(e^{-[\sigma+\eta\gamma(1-q_+)]\tau_a}-e^{-[\sigma+\eta\gamma(1-q_+)]\tau_b})}{\sigma+\eta\gamma(1-q_+)}\right\}, \tag{E7}$$

where we have taken the limit $\epsilon \to 0$. We note then that the asymptotic forms of $E(\sigma)$, $C(\sigma)$, and $D(\sigma)$ for large γ are given by

$$E(\sigma) \sim \frac{1}{\sigma+\gamma\eta+W_{-,+}}, \quad C(\sigma) \sim \frac{\gamma\eta - W_{-,+}\left(\frac{1}{a}-\frac{1}{b}\right)}{\sigma+\gamma\eta+W_{-,+}}, \quad D(\sigma) \sim \frac{W_{-,+}\left(\frac{1}{a}-\frac{1}{b}\right)}{\sigma+\gamma\eta+W_{-,+}}. \tag{E8}$$

Then Eq. (51) follows.

3. Collapse-measurement setup

We derive the explicit expressions for the functions $C(\sigma)$, $D(\sigma)$, and $E(\sigma)$ (and their asymptotic forms for large γ) to determine the generating function of the distribution of spikes for the collapse-measurement case. Thanks to Eq. (59) we have that

$$E(\sigma) = \frac{1}{\gamma_1\eta_1+\gamma_2}\left\{\frac{\gamma_2(1-\eta_2)(1-e^{-\sigma\tau})}{\sigma} + \frac{(\gamma_1\eta_1+\gamma_2\eta_2)(1-e^{-(\sigma+\gamma_2+\gamma_1\eta_1)\tau})}{\sigma+\gamma_2+\gamma_1\eta_1}\right\}, \tag{E9}$$

$$C(\sigma)+D(\sigma) = \frac{\gamma_1\eta_1(1-e^{-(\sigma+\gamma_2+\gamma_1\eta_1)\tau})}{\sigma+\gamma_1\eta_1+\gamma_2}, \tag{E10}$$

and

$$D(\sigma) = \frac{\gamma_1\eta_1(e^{-(\sigma+\gamma_1\eta_1+\gamma_2)\tau_a}-e^{-(\sigma+\gamma_1\eta_1+\gamma_2)\tau_b})}{\sigma+\gamma_1\eta_1+\gamma_2}. \tag{E11}$$

We note then that the asymptotic forms of $E(\sigma)$, $C(\sigma)$, and $D(\sigma)$ for large γ_1 are given by

$$E(\sigma) \sim \frac{1-\frac{\epsilon\gamma_2(1-\eta_2)}{\sigma+\gamma_1\eta_1+\gamma_2}}{\sigma+\gamma_1\eta_1+\gamma_2}, \quad C(\sigma) \sim \frac{\gamma_1\eta_1-\gamma_2(1-\eta_2)\left(\epsilon+\frac{1}{a}-\frac{1}{b}\right)}{\sigma+\gamma_1\eta_1+\gamma_2}, \quad D(\sigma) \sim \frac{\gamma_2(1-\eta_2)\left(\frac{1}{a}-\frac{1}{b}\right)}{\sigma+\gamma_1\eta_1+\gamma_2}. \tag{E12}$$

Then Eq. (60) follows by taking the limit $\gamma_1 \to \infty$ and $\epsilon \to 0$, in that order.

APPENDIX F: NUMERICAL METHODS

Here, we discuss the two numerical methods employed to simulate the 1D stochastic differential equations (SDEs) with Poissonian noise that govern the evolution of the state x_t. The first method is a first-order iterative approach where, given an SDE with Poissonian noise,

$$\begin{aligned} dx_t &= f(x_t)dt + h(x_t)d\mathcal{N}_t, \\ d\mathcal{N}_t d\mathcal{N}_t &= d\mathcal{N}_t, \\ \mathbb{E}[d\mathcal{N}_t] &= g(x_t)dt, \end{aligned} \tag{F1}$$

where $\{x_t\}_{t=\Delta t, 2\Delta t \ldots}$ is obtained using the rule

$$x_{t+\Delta t} = x_t + f(x_t)\Delta t + h(x_t)r_t, \tag{F2}$$

where the step size $\Delta t \ll 1$ is chosen appropriately and the random number r_t is sampled from a Bernoulli distribution with the parameter $p = g(x_t)\Delta t$.

The second method is based on the principle that the stochastic evolution equation (F1) is composed of deterministic flows and jumps (not to be confused with quantum jumps). Discarding the Poissonian noise, Eq. (F1) becomes a first-order ordinary differential equation (ODE): $\dot{x}_t = f(x_t)$ which, given the initial condition $x_{t=0} = x_0$, has the unique solution x_{t,x_0}. Now, the probability $\nu(t, x_0)$ of having no jumps in an interval $(0, t)$ with the initial condition $x_{t=0} = x_0$ is formally given by

$$\nu(t, x_0) = \exp\left(-\int_{x_0}^{x_{t,x_0}} \frac{g(x)dx}{f(x)}\right). \tag{F3}$$

We now have all the ingredients necessary for this method. Given that the state at time t_i is x_{t_i}, the algorithm for time evolution is as follows:

(1) Choose a random number τ from the distribution $-\frac{\partial \nu(t,x_{t_i})}{\partial t}$, where $\nu(t,x_{t_i})$ is given by Eq. (F3). Physically speaking, this means that a jump has occurred at time $t_{i+1} = t_i + \tau$ and from the deterministic flow, we know the state takes the values $x_{t'} = x_{t'-t_i,x_{t_i}}$ for $t_i \leqslant t' < t_{i+1}$.

(2) The value of the state at time t_{i+1} is set by $x_{t_{i+1}} = x_{\tau,x_{t_i}} + h(x_{\tau,x_{t_i}})$.

(3) Repeat steps 1 and 2 with the transformations $t_i \to t_{i+1}$ and $t_{i+1} \to t_{i+2}$.

[1] D. Bohm and J. Bub, A proposed solution of the measurement problem in quantum mechanics by a hidden variable theory, Rev. Mod. Phys. **38**, 453 (1966).

[2] P. Pearle, Reduction of the state vector by a nonlinear Schrödinger equation, Phys. Rev. D **13**, 857 (1976).

[3] P. Pearle, Stochastic dynamical reduction theories and superluminal communication, Phys. Rev. D **33**, 2240 (1986).

[4] L. Diósi, Stochastic pure state representation for open quantum systems, Phys. Lett. A **114**, 451 (1986).

[5] N. Gisin, Quantum measurements and stochastic processes, Phys. Rev. Lett. **52**, 1657 (1984).

[6] A. Barchielli, Measurement theory and stochastic differential equations in quantum mechanics, Phys. Rev. A **34**, 1642 (1986).

[7] R. Alicki and M. Fannes, On dilating quantum dynamical semigroups with classical Brownian motion, Lett. Math. Phys. **11**, 259 (1986).

[8] L. Diósi, Continuous quantum measurement and Itô formalism, Phys. Lett. A **129**, 419 (1988).

[9] V. P. Belavkin, A new wave equation for a continuous nondemolition measurement, Phys. Lett. A **140**, 355 (1989).

[10] V. P. Belavkin, A posterior Schrödinger equation for continuous nondemolition measurement, J. Math. Phys. **31**, 2930 (1990).

[11] A. Barchielli and V. P. Belavkin, Measurements continuous in time and a posteriori states in quantum mechanics, J. Phys. A: Math. Gen. **24**, 1495 (1991).

[12] V. P. Belavkin, Quantum continual measurements and a posteriori collapse on CCR, Commun. Math. Phys. **146**, 611 (1992).

[13] P. Staszewski, Viacheslav Pavlovich Belavkin, 1946–2012: In memory of Professor V. P. Belavkin, Open Syst. Inf. Dyn. **20**, 1377001 (2013).

[14] M. Holland, S. Marksteiner, P. Marte, and P. Zoller, Measurement induced localization from spontaneous decay, Phys. Rev. Lett. **76**, 3683 (1996).

[15] C. W. Gardiner, A. S. Parkins, and P. Zoller, Wave-function quantum stochastic differential equations and quantum-jump simulation methods, Phys. Rev. A **46**, 4363 (1992).

[16] J. Dalibard, Y. Castin, and K. Mølmer, Wave-function approach to dissipative processes in quantum optics, Phys. Rev. Lett. **68**, 580 (1992).

[17] H. M. Wiseman and G. J. Milburn, Quantum theory of field-quadrature measurements, Phys. Rev. A **47**, 642 (1993).

[18] B. M. Garraway and P. L. Knight, Evolution of quantum superpositions in open environments: Quantum trajectories, jumps, and localization in phase space, Phys. Rev. A **50**, 2548 (1994).

[19] C. W. Gardiner and P. Zoller, *Quantum Noise: A Handbook of Markovian and Non-Markovian Quantum Stochastic Methods with Applications to Quantum Optics*, 3rd ed., Springer Series in Synergetics (Springer, Berlin, 2004), pp. xxii, 449.

[20] H. M. Wiseman and G. J. Milburn, *Quantum Measurement and Control* (Cambridge University Press, Cambridge, 2010), pp. xvi, 460.

[21] S. Haroche and J.-M. Raimond, *Exploring the Quantum: Atoms, Cavities, and Photons*, Oxford Graduate Texts (Oxford University Press, Oxford, 2006), pp. x, 605.

[22] H.-P. Breuer and F. Petruccione, *The Theory of Open Quantum Systems* (Oxford University Press, New York, 2002), pp. xxii, 625.

[23] H. Carmichael, *An Open Systems Approach to Quantum Optics*, Lecture Notes in Physics Monographs, Vol. 18 (Springer, New York, 2009).

[24] K. Jacobs, *Quantum Measurement Theory and its Applications* (Cambridge University Press, Cambridge, 2014).

[25] C. Guerlin, J. Bernu, S. Deleglise, C. Sayrin, S. Gleyzes, S. Kuhr, M. Brune, J.-M. Raimond, and S. Haroche, Progressive field-state collapse and quantum non-demolition photon counting, Nature (London) **448**, 889 (2007).

[26] S. Gleyzes, S. Kuhr, C. Guerlin, J. Bernu, S. Deleglise, U. Busk Hoff, M. Brune, J.-M. Raimond, and S. Haroche, Quantum jumps of light recording the birth and death of a photon in a cavity, Nature (London) **446**, 297 (2007).

[27] C. Sayrin, I. Dotsenko, X. Zhou, B. Peaudecerf, T. Rybarczyk, S. Gleyzes, P. Rouchon, M. Mirrahimi, H. Amini, M. Brune *et al.*, Real-time quantum feedback prepares and stabilizes photon number states, Nature (London) **477**, 73 (2011).

[28] K. Murch, S. Weber, K. Beck, E. Ginossar, and I. Siddiqi, Reduction of the radiative decay of atomic coherence in squeezed vacuum, Nature (London) **499**, 62 (2013).

[29] K. W. Murch, S. Weber, C. Macklin, and I. Siddiqi, Observing single quantum trajectories of a superconducting quantum bit, Nature (London) **502**, 211 (2013).

[30] S. Weber, A. Chantasri, J. Dressel, A. N. Jordan, K. W. Murch, and I. Siddiqi, Mapping the optimal route between two quantum states, Nature (London) **511**, 570 (2014).

[31] S. L. Adler, D. C. Brody, T. A. Brun, and L. P. Hughston, Martingale models for quantum state reduction, J. Phys. A: Math. Gen. **34**, 8795 (2001).

[32] R. van Handel, J. K. Stockton, and H. Mabuchi, Feedback control of quantum state reduction, IEEE Trans. Automat. Control **50**, 768 (2005).

[33] H. Maassen and B. Kümmerer, Purification of quantum trajectories, *Dynamics & Stochastics*, IMS Lecture Notes Monographs Series, Vol. 48 (Inst. Math. Statist., Beachwood, OH, 2006), pp. 252–261.

[34] M. Bauer and D. Bernard, Convergence of repeated quantum nondemolition measurements and wave-function collapse, Phys. Rev. A **84**, 044103 (2011).

[35] T. Benoist and C. Pellegrini, Large time behavior and convergence rate for quantum filters under standard non demolition conditions, Commun. Math. Phys. **331**, 703 (2014).

[36] N. Bohr, I. on the constitution of atoms and molecules, London, Edinburgh, Dublin Philos. Mag., J. Sci. **26**, 1 (1913).

[37] W. Nagourney, J. Sandberg, and H. Dehmelt, Shelved optical electron amplifier: Observation of quantum jumps, Phys. Rev. Lett. **56**, 2797 (1986).

[38] T. Sauter, W. Neuhauser, R. Blatt, and P. E. Toschek, Observation of quantum jumps, Phys. Rev. Lett. **57**, 1696 (1986).

[39] M. Bauer, D. Bernard, and A. Tilloy, Computing the rates of measurement-induced quantum jumps, J. Phys. A: Math. Theor. **48**, 25FT02 (2015).

[40] T. Benoist, C. Bernardin, R. Chetrite, R. Chhaibi, J. Najnudel, and C. Pellegrini, Emergence of jumps in quantum trajectories via homogenization, Commun. Math. Phys. **387**, 1821 (2021).

[41] M. Ballesteros, N. Crawford, M. Fraas, J. Fröhlich, and B. Schubnel, Perturbation theory for weak measurements in quantum mechanics, systems with finite-dimensional state space, Ann. Henri Poincaré **20**, 299 (2019).

[42] A. Degasperis, L. Fonda, and G. C. Ghirardi, Does the lifetime of an unstable system depend on the measuring apparatus? Nuovo Cimento A **21**, 471 (1974).

[43] B. Misra and E. C. G. Sudarshan, The Zeno's paradox in quantum theory, J. Math. Phys. **18**, 756 (1977).

[44] A. Peres, Measurement of time by quantum clocks, Am. J. Phys. **48**, 552 (1980).

[45] W. M. Itano, D. J. Heinzen, J. J. Bollinger, and D. J. Wineland, Quantum zeno effect, Phys. Rev. A **41**, 2295 (1990).

[46] C. Teuscher, Turing's connectionism, *Alan Turing: Life and Legacy of a Great Thinker* (Springer, Berlin, 2004), pp. 499–529.

[47] D. Layden, E. Martín-Martínez, and A. Kempf, Perfect zeno-like effect through imperfect measurements at a finite frequency, Phys. Rev. A **91**, 022106 (2015).

[48] N. Gisin and I. C. Percival, The quantum-state diffusion model applied to open systems, J. Phys. A: Math. Gen. **25**, 5677 (1992).

[49] H. Mabuchi and H. M. Wiseman, Retroactive quantum jumps in a strongly coupled atom-field system, Phys. Rev. Lett. **81**, 4620 (1998).

[50] J. D. Cresser, S. M. Barnett, J. Jeffers, and D. T. Pegg, Measurement master equation, Opt. Commun. **264**, 352 (2006).

[51] A. J. Colin, S. M. Barnett, and J. Jeffers, Measurement-driven dynamics for a coherently-excited atom, J. Mod. Opt. **59**, 1803 (2012).

[52] M. Bauer, D. Bernard, and A. Tilloy, Zooming in on quantum trajectories, J. Phys. A: Math. Theor. **49**, 10LT01 (2016).

[53] A. Tilloy, M. Bauer, and D. Bernard, Spikes in quantum trajectories, Phys. Rev. A **92**, 052111 (2015).

[54] M. Bauer and D. Bernard, Stochastic spikes and strong noise limits of stochastic differential equations, Ann. Henri Poincaré **19**, 653 (2018).

[55] M. Kolb and M. Liesenfeld, Stochastic spikes and Poisson approximation of one-dimensional stochastic differential equations with applications to continuously measured quantum systems, Ann. Henri Poincaré **20**, 1753 (2019).

[56] C. Bernardin, R. Chetrite, R. Chhaibi, J. Najnudel, and C. Pellegrini, Spiking and collapsing in large noise limits of sdes, Ann. Appl. Probab. **33**, 417 (2023).

[57] A. Tilloy, Continuous collapse models on finite dimensional hilbert spaces, *Do Wave Functions Jump?* (Springer, Cham, 2020), pp. 167–188.

[58] M. R. Evans and S. N. Majumdar, Diffusion with stochastic resetting, Phys. Rev. Lett. **106**, 160601 (2011).

[59] M. R. Evans and S. N. Majumdar, Diffusion with optimal resetting, J. Phys. A: Math. Theor. **44**, 435001 (2011).

[60] M. R. Evans, S. N. Majumdar, and G. Schehr, Stochastic resetting and applications, J. Phys. A: Math. Theor. **53**, 193001 (2020).

[61] A. Pal, A. Kundu, and M. R. Evans, Diffusion under time-dependent resetting, J. Phys. A: Math. Theor. **49**, 225001 (2016).

[62] V. Gorini, A. Kossakowski, and E. C. G. Sudarshan, Completely positive dynamical semigroups of *N*-level systems, J. Math. Phys. **17**, 821 (1976).

[63] G. Lindblad, On the generators of quantum dynamical semigroups, Commun. Math. Phys. **48**, 119 (1976).

[64] C. Pellegrini, Existence, uniqueness and approximation of a stochastic Schrödinger equation: the diffusive case, Ann. Probab. **36**, 2332 (2008).

[65] K. Snizhko, P. Kumar, and A. Romito, Quantum zeno effect appears in stages, Phys. Rev. Res. **2**, 033512 (2020).

[66] V. Dubey, R. Chetrite, and A. Dhar, Quantum resetting in continuous measurement induced dynamics of a qubit, J. Phys. A: Math. Theor. **56**, 154001 (2023).

[67] V. B. Braginskĭ and Y. I. Vorontsov, Quantum-mechanical limitations in macroscopic experiments and modern experimental technique, Usp. Fiz. Nauk **114**, 41 (1974) [Sov. Phys. Usp. **17**, 644 (1975)].

[68] K. S. Thorne, R. W. P. Drever, C. M. Caves, M. Zimmermann, and V. D. Sandberg, Quantum nondemolition measurements of harmonic oscillators, Phys. Rev. Lett. **40**, 667 (1978).

[69] W. G. Unruh, Quantum nondemolition, in *Gravitational Radiation, Collapsed Objects and Exact Solutions (Proceedings of the Einstein Centenary Summer School, Perth, 1979)*, Lecture Notes in Physics, Vol. 124 (Springer, Berlin, 1980), pp. 385–426.

[70] V. B. Braginsky, Y. I. Vorontsov, and K. S. Thorne, Quantum nondemolition measurements, Science **209**, 547 (1980).

[71] C. M. Caves, K. S. Thorne, R. W. Drever, V. D. Sandberg, and M. Zimmermann, On the measurement of a weak classical force coupled to a quantum-mechanical oscillator. I. Issues of principle, Rev. Mod. Phys. **52**, 341 (1980).

[72] G. J. Milburn and D. F. Walls, Quantum nondemolition measurements via quadratic coupling, Phys. Rev. A **28**, 2065 (1983).

[73] W. H. Zurek, Pointer basis of quantum apparatus: into what mixture does the wave packet collapse? Phys. Rev. D **24**, 1516 (1981).

[74] É. Roldán, I. Neri, R. Chetrite, S. Gupta, S. Pigolotti, F. Jülicher, and K. Sekimoto, Martingales for physicists: a treatise on stochastic thermodynamics and beyond, Adv. Phys. **72**, 1 (2023).

[75] R. Feynman, R. Leighton, and M. Sands, *The Feynman Lectures on Physics* (Addison-Wesley, Boston, 1964), Vol. II, Chap. 35.

[76] M. Le Bellac, in *Quantum Physics*, edited by P. d. Forcrand-Millard (Cambridge University Press, Camb ridge, 2006).

[77] E. B. Davies, *Quantum Theory of Open Systems* (Academic, London, 1976), pp. x, 171.

[78] G. de Lange, D. Ristè, M. J. Tiggelman, C. Eichler, L. Tornberg, G. Johansson, A. Wallraff, R. N. Schouten, and L. DiCarlo, Reversing quantum trajectories with analog feedback, Phys. Rev. Lett. **112**, 080501 (2014).

[79] Z. K. Minev, S. O. Mundhada, S. Shankar, P. Reinhold, R. Gutiérrez-Jáuregui, R. J. Schoelkopf, M. Mirrahimi, H. J. Carmichael, and M. H. Devoret, To catch and reverse a quantum jump mid-flight, Nature (London) **570**, 200 (2019).

[80] D. Applebaum, Levy processes and stochastic calculus, Cambridge Studies Adv. Math. **116**, 223 (2009).

[81] P. Tankov, *Financial Modelling with Jump Processes* (CRC Press, Boca Raton, FL, 2003).